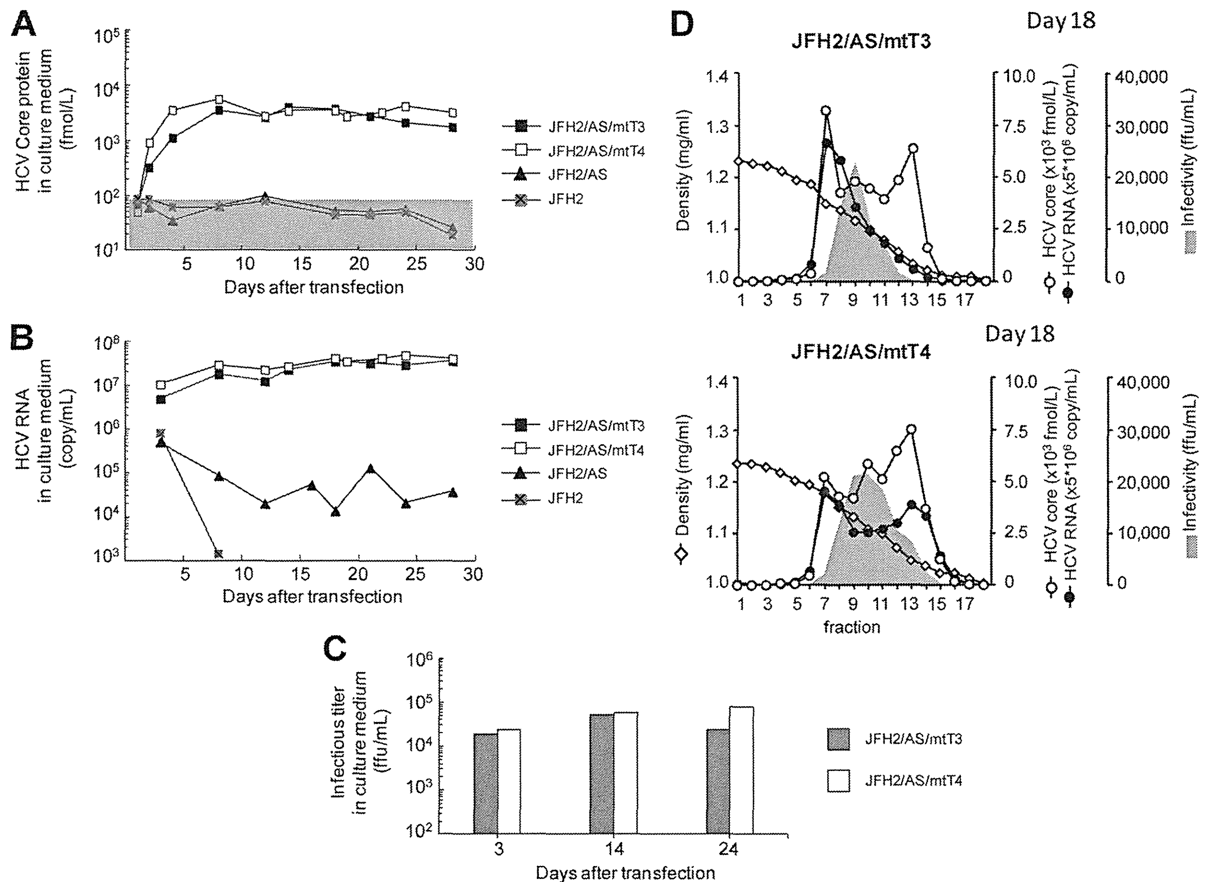

FIG 14 Full-length RNA was synthesized from the JFH2 construct and its derivatives with mutations. RNA-transfected cells were serially passaged, and culture supernatants were harvested at the indicated time points. HCV core protein (A), HCV RNA (B), and infectivity (C) levels in the culture media were determined. The data in the gray area were below the detection limit of the assay to detect HCV core protein. (D) Density gradient analysis of culture supernatant from JFH2/AS cell-culture adapted virus-infected Huh-7.5.1 cells. Culture supernatants of Huh-7.5.1 cells infected with JFH2/mtT3 and JFH2/mtT4 viruses were harvested 18 days after inoculation. Assays were performed as described in the legend of Fig. 6E. Open diamond, buoyant density.

medium than JFH-1. J6/JFH2/AS/mtT1A, J6/JFH2/AS/mtT1B, JFH2/AS/mtT3, and JFH2/AS/mtT4 RNA-transfected cells showed different percentages of secreted core protein. mtT1A and mtT1B constructs showed similar replication levels (Fig. 15B), but mtT1B showed a higher percentage of core protein secretion than mtT1A (Fig. 15C). mtT3 and mtT4 showed similar percentages of core protein secretion, which are higher than the level of JFH1 (Fig. 15C). Because J6/JFH2/AS RNA-transfected cells did not secrete core protein despite intracellular core protein expression (Fig. 15A and B), the adaptive mutant constructs obtained core protein (or virus particle) secretion phenotypes. Thus, during the adaptation process, the viruses obtained both higher replication capacity and core protein secretion capacity by their adaptive mutations.

Other HCV constructs with the 2217AS mutation. The alanine residue at amino acid position 2217 is located in the ISDR of NS5A, and it is conserved among HCV strains including genotype 1 and 2 strains. Because the 2217AS mutation in NS5A is the key mutation for the production of cell culture-adapted HCV, we introduced this mutation into other wild-type HCV constructs, i.e., H77 (genotype 1a), Con1 (genotype 1b), and J6CF (genotype 2a). Synthetic RNAs including the 2217AS mutation were electroporated into Huh-7.5.1 cells, and then the transfected cells were serially passaged. HCV core protein secretion was measured in the culture medium of transfected cells. However, we could not observe the increment of HCV core levels in the culture medium (data not shown). Therefore, we concluded that the 2217AS mutation does not always induce cell culture adaptation in HCV isolates.

DISCUSSION

In previous studies, we have isolated cell culture-infectious HCV, the JFH-1 strain, from a patient with fulminant hepatitis (14, 38). In this report, we isolated another HCV cDNA, named JFH-2, also from a fulminant hepatitis patient. We constructed a subgenomic replicon with the JFH-2 sequence, but its replication efficiency was low. Among the mutations found in the replicon genome, the 2217AS mutation in the ISDR exhibited the strongest adaptive effect. Interestingly, the full-length chimeric or wild-type JFH-2 genome with adaptive mutations could replicate and produce infectious virus particles. Virus infection efficiency was sufficient for autonomous virus propagation in cultured cells.

Several full-length HCV cDNAs have been cloned, and their infectivity has been confirmed *in vivo* with chimpanzee models (18, 39). However, it has been difficult to produce recombinant viral particles and test their infectivity by using cell culture

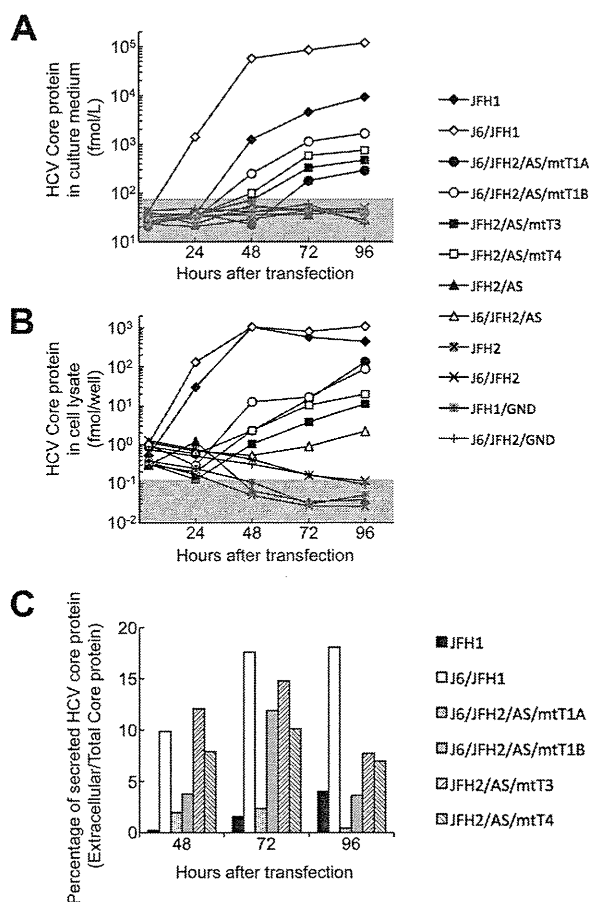

FIG 15 Transient virus production assay of J6/JFH2- and JFH2-related constructs with CD81-defective Huh7-25 cells. Full-length HCV RNA was synthesized from the JFH1, J6/JFH1, JFH2, and J6/JFH2 constructs and their derivatives with mutations and transfected into Huh7-25 cells. (A) HCV core protein levels in culture medium were determined at 4, 24, 48, 72, and 96 h after transfection. The data in the gray area were below detection limit. (B) HCV core protein levels in the cell lysate were determined at 24, 48, 72, and 96 h after transfection. (C) Percentages of secreted HCV core protein from the transfected cells were determined at 48, 72, and 96 h after transfection. Percentages of secreted HCV core protein were calculated only for the indicated viruses. All assays were performed in duplicate, and the data represent average values.

systems (4, 28). Only the JFH-1 strain efficiently replicates in HuH-7 cells and other hepatic and nonhepatic cell lines in subgenomic replicon form (20, 38, 41). Full-length wild-type JFH-1 RNA and chimeric JFH-1 RNA can replicate in HuH-7 cells and produce infectious virus. Since the JFH-1 strain was isolated from a patient with fulminant hepatitis, we assumed that virus strains that cause fulminant hepatitis may replicate efficiently in cultured cells. To identify more HCV clones that can replicate in cultured cells, we isolated the JFH-2 strain from another fulminant hepatitis patient (15). Interestingly, the JFH-2 strain showed a low level of replication in cultured cells in the initial subgenomic replicon experiment. This result may suggest that HCV strains isolated from fulminant hepatitis patients are able to replicate more efficiently than strains from chronic hepatitis patients; however, this hypothesis should be confirmed by testing more HCV strains from patients with fulminant hepatitis. The JFH-2 patient received a course of betamethasone therapy and developed fulminant hepatitis after the withdrawal of betamethasone. It is thus possible that the JFH-2 strain obtained its higher replication capacity in the immune-suppressed host environment. To confirm this hypothesis, we must test the replication efficiency of HCV strains isolated from other immune-suppressed patients, such as patients who are coinfected with HIV, patients who are reinfected after a transplant, and patients who are treated with immunosuppressive agents.

In previous reports, adaptive mutations have been found to enhance viral RNA replication at the expense of virus particle formation efficiency (28). A highly cell culture-adapted Con1 strain can replicate in cultured cells, but it cannot produce infectious virus particles. Interestingly, a highly adapted Con1 strain was not infectious for chimpanzees, while moderately adapted Con1 was infectious. However, the virus recovered from the infected animal was wild-type Con1 virus (5). This result clearly suggests that HCV strains with lower replication efficiencies are favorable for *in vivo* infection. However, we must note that the "replication efficiency" is determined in cultured cells. In the case of JFH-2, we found several adaptive mutations in the subgenomic replicon clones, and the most adaptive mutation, 2217AS, was tested in full-length HCV replication and virus production. After the RNA transfection of J6/JFH2/AS, we could not detect substantial virus secretion for about 30 days. However, after 30 days, significant levels of infectious virus particles were secreted into the culture medium. Naive Huh-7.5.1 cells were inoculated three times with the cell culture-adapted virus. This virus adaptation was also tested with full-length JFH2/AS, and we successfully obtained infectious JFH2/AS virus. Both the J6/JFH2/AS and JFH2/AS viruses acquired the ability for autonomous virus expansion in Huh-7.5.1 cells, and several additional mutations were found in their genomes. Interestingly, the 2695TI mutation in NS5B was commonly found in all of the adapted virus genomes, and isoleucine at amino acid position 2695 is also found in the JFH-1 strain. However, the introduction of only the 2695TI mutation into the J6/JFH2/AS or JFH2/AS virus genome did not restore robust virus production (data not shown). After repeated virus passages, mutations were found throughout the viral genome (in J6/JFH2/AS-T1Ai3 and -T1Bi3 and in JFH2/AS-T3i3 and -T4i3), and we are currently investigating which mutations or combinations of mutations are most important for this adaptation. From the comparisons of cell culture-adapted viruses and their parental virus constructs, adaptive mutations are necessary to increase both viral genome replication and virus particle assembly/secretion efficiency (Fig. 15). The procedure to produce cell culture-adapted HCV was thus established. The adaptive mutations found from the subgenomic replicon assay were introduced into the full-length genome, and the cells transfected with virus RNA were repeatedly passaged until the virus particles were produced.

In vivo infectivity may be inversely related to the replication efficiency in cultured cells, as discussed above. The original JFH-2 patient serum was infectious in human liver-transplanted mice; however, cell culture-adapted J6/JFH2/AS virus was not infectious. The JFH-1 virus was infectious not only for cultured cells but also for chimpanzees and human liver-transplanted mice (10, 38). However, the JFH-1 infection in chimpanzees was only mild and transient without any liver pathology. Thus, the J6/JFH2/AS and JFH2/AS viruses are more cell culture-adapted and attenuated than the JFH-1 virus. It may be worthwhile to test this cell culture-

Downloaded from http://jvi.asm.org/ on March 4, 2013 by NATL INST OF INFECTIOUS DISEAS

adapted strain as a live attenuated vaccine candidate to induce protective immunity. However, for ethical reasons, the necessary chimpanzee experiments are not appropriate to perform. Therefore, we should wait for the establishment of immunocompetent small-animal models susceptible to HCV infection to perform this kind of study. Furthermore, future studies should examine the *in vivo* infectivity of the adapted J6/JFH2 and JFH2 viruses isolated in the present study.

The 2217AS mutation is located in the ISDR. In the previous study of the genotype 1b subgenomic replicon, mutations introduced into the ISDR enhanced the colony formation efficiency of the HCV replicons (17, 23). However, mutations in the ISDR impaired the genotype 1b HCV replication in human liver-transplanted mice (9). The exact mechanism of the ISDR is still not clear although the number of mutations in the ISDR is related to the efficacy of interferon therapy (8). Our results in this study also support the concept that the 2217AS mutation in the ISDR enhances replicon replication efficiency although the J6/JFH2/AS virus did not infect human liver-transplanted mice. Further studies are necessary to understand the molecular mechanism of the effects of adaptive mutations in the ISDR.

In the present study, we established a cell culture-adapted HCV strain, JFH-2. The virus could be passaged continuously in naive Huh-7.5.1 cells. This approach may be applicable to the establishment of new infectious HCV clones. Novel antiviral drugs are under development, and some of them will be used in the clinical setting. However, most of them target genotype 1 HCV strains. To eradicate other genotypes of HCV, it is important to establish their replicons and infectious virus culture systems.

ACKNOWLEDGMENTS

Huh-7.5.1 cells were kindly provided by Francis V. Chisari. The J6CF plasmid was a kind gift from Jens Bukh. Anti-HCV human IgG was a kind gift from Hiroshi Yoshizawa and Junko Tanaka, Hiroshima University. AP33 antibody was generously provided by Genentec. We thank Tetsuro Suzuki and Hideki Aizaki for their helpful discussions. We also thank Minako Kaga for her technical assistance.

This work was partially supported by Grants-in-Aid for Scientific Research from the Japan Society for the Promotion of Science, from the Ministry of Health, Labor and Welfare of Japan, from the Ministry of Education, Culture, Sports, Science and Technology, from the National Institute of Biomedical Innovation, and by the Research on Health Sciences Focusing on Drug Innovation from the Japan Health Sciences Foundation.

REFERENCES

1. **Aizaki H, et al.** 2008. Critical role of virion-associated cholesterol and sphingolipid in hepatitis C virus infection. J. Virol. **82**:5715–5724.
2. **Akazawa D, et al.** 2007. CD81 expression is important for the permissiveness of Huh7 cell clones for heterogeneous hepatitis C virus infection. J. Virol. **81**:5036–5045.
3. **Akazawa D, et al.** 2011. Production and characterization of HCV particles from serum-free culture. Vaccine **29**:4821–4828.
4. **Bartenschlager R, Lohmann V.** 2000. Replication of hepatitis C virus. J. Gen. Virol. **81**:1631–1648.
5. **Bukh J, et al.** 2002. Mutations that permit efficient replication of hepatitis C virus RNA in Huh-7 cells prevent productive replication in chimpanzees. Proc. Natl. Acad. Sci. U. S. A. **99**:14416–14421.
6. **Choo QL, et al.** 1989. Isolation of a cDNA clone derived from a blood-borne non-A non-B viral hepatitis genome. Science **244**:359–362.
7. **Di Bisceglie AM, Hoofnagle JH.** 2002. Optimal therapy of hepatitis C. Hepatology **36**:S121–S127.
8. **Enomoto N, et al.** 1995. Sensitivity to interferon is conferred by amino acid substitutions in the NS5A region. J. Clin. Invest. **96**:224–230.
9. **Hiraga N, et al.** 2011. Impact of viral amino acid substitutions and host interleukin-28b polymorphism on replication and susceptibility to interferon of hepatitis C virus. Hepatology **54**:764–771.
10. **Kato T, et al.** 2008. Hepatitis C virus JFH-1 strain infection in chimpanzees is associated with low pathogenicity and emergence of an adaptive mutation. Hepatology **48**:732–740.
11. **Kato T, et al.** 2003. Efficient replication of the genotype 2a hepatitis C virus subgenomic replicon. Gastroenterology **125**:1808–1817.
12. **Kato T, et al.** 2005. Detection of anti-hepatitis C virus effects of interferon and ribavirin by a sensitive replicon system. J. Clin. Microbiol. **43**:5679–5684.
13. **Kato T, et al.** 2006. Cell culture and infection system for hepatitis C virus. Nat. Protoc. **1**:2334–2339.
14. **Kato T, et al.** 2001. Sequence analysis of hepatitis C virus isolated from a fulminant hepatitis patient. J. Med. Virol. **64**:334–339.
15. **Kato T, et al.** 2003. Processing of hepatitis C virus core protein is regulated by its C-terminal sequence. J. Med. Virol. **69**:357–366.
16. **Kiyosawa K, et al.** 1990. *Interrelationship of blood transfusion, non-A, non-B hepatitis and hepatocellular carcinoma: analysis by detection of antibody to hepatitis C virus.* Hepatology **12**:671–675.
17. **Kohashi T, et al.** 2006. Site-specific mutation of the interferon sensitivity-determining region (ISDR) modulates hepatitis C virus replication. J. Viral Hepat. **13**:582–590.
18. **Kolykhalov AA, et al.** 1997. Transmission of hepatitis C by intrahepatic inoculation with transcribed RNA. Science **277**:570–574.
19. **Kuo G, et al.** 1989. An assay for circulating antibodies to a major etiologic virus of human non-A non-B hepatitis. Science **244**:362–364.
20. **Lindenbach BD, et al.** 2005. Complete replication of hepatitis C virus in cell culture. Science **309**:623–626.
21. **Lindenbach BD, et al.** 2006. Cell culture-grown hepatitis C virus is infectious in vivo and can be recultured in vitro. Proc. Natl. Acad. Sci. U. S. A. **103**:3805–3809.
22. **Lohmann V, et al.** 1999. Replication of subgenomic hepatitis C virus RNAs in a hepatoma cell line. Science **285**:110–113.
23. **Maekawa S, et al.** 2004. Introduction of NS5A mutations enables subgenomic HCV replicon derived from chimpanzee-infectious HC-J4 isolate to replicate efficiently in Huh-7 cells. J. Viral Hepat. **11**:394–403.
24. **McHutchison JG, et al.** 1998. Interferon alfa-2b alone or in combination with ribavirin as initial treatment for chronic hepatitis C. N. Engl. J. Med. **339**:1485–1492.
25. **Merck & Co.** 2011. *Victrelis (boceprevir) prescribing information.* Merck & Co., Whitehouse Station, NJ. http://www.accessdata.fda.gov/drugsatfda_docs/label/2011/202258lbl.pdf.
26. **Murayama A, et al.** 2007. The NS3 helicase and NS5B-to-3′X regions are important for efficient hepatitis C virus strain JFH-1 replication in Huh7 cells. J. Virol. **81**:8030–8040.
27. **Murayama A, et al.** 2010. RNA polymerase activity and specific RNA structure are required for efficient HCV replication in cultured cells. PLoS Pathog. **6**:e1000885. doi:10.1371/journal.ppat.1000885.
28. **Pietschmann T, et al.** 2002. Persistent and transient replication of full-length hepatitis C virus genomes in cell culture. J. Virol. **76**:4008–4021.
29. **Pietschmann T, et al.** 2009. Production of infectious genotype 1b virus particles in cell culture and impairment by replication enhancing mutations. PLoS Pathog. **5**:e1000475. doi:10.1371/journal.ppat.1000475.
30. **Poynard T, et al.** 1998. Randomised trial of interferon α2b plus ribavirin for 48 weeks or for 24 weeks versus interferon α2b plus placebo for 48 weeks for treatment of chronic infection with hepatitis C virus. Lancet **352**:1426–1432.
31. **Saeed M, et al.** 2009. Evaluation of hepatitis C virus core antigen assays in detecting recombinant viral antigens of various genotypes. J. Clin. Microbiol. **47**:4141–4143.
32. **Takahashi H, et al.** 2010. Biological properties of purified recombinant HCV particles with an epitope-tagged envelope. Biochem. Biophys. Res. Commun. **395**:565–571.
33. **Tateno C, et al.** 2004. Near completely humanized liver in mice shows human-type metabolic responses to drugs. Am. J. Pathol. **165**:901–912.
34. **U. S. Food and Drug Administration.** 2011. FDA news release. FDA approves Incivek for hepatitis C. U.S. Food and Drug Administration, Silver Spring, MD. http://www.fda.gov/NewsEvents/Newsroom/PressAnnouncements/ucm256299.htm.
35. **U. S. Food and Drug Administration.** 2011. FDA news release. FDA approves Victrelis for hepatitis C. U.S. Food and Drug Administration,

Silver Spring, MD. http://www.fda.gov/NewsEvents/Newsroom/PressAnnouncements/ucm255390.htm.
36. **Vertex Pharmaceuticals.** 2011. Incivek (telaprevir) prescribing information. Vertex Pharmaceuticals, Cambridge, MA. http://www.accessdata.fda.gov/drugsatfda_docs/label/2011/201917lbl.pdf.
37. **Wakita T.** 2009. Isolation of JFH-1 strain and development of an HCV infection system. Methods Mol. Biol. 510:305–327.
38. **Wakita T, et al.** 2005. Production of infectious hepatitis C virus in tissue culture from a cloned viral genome. Nat. Med. 11:791–796.
39. **Yanagi M, Purcell RH, Emerson SU, Bukh J.** 1997. Transcripts from a single full-length cDNA clone of hepatitis C virus are infectious when directly transfected into the liver of a chimpanzee. Proc. Natl. Acad. Sci. U. S. A. 94:8738–8743.
40. **Yanagi M, Purcell RH, Emerson SU, Bukh J.** 1999. Hepatitis C virus: an infectious molecular clone of a second major genotype (2a) and lack of viability of intertypic 1a and 2a chimeras. Virology 262:250–263.
41. **Zhong JP, et al.** 2005. Robust hepatitis C virus infection in vitro. Proc. Natl. Acad. Sci. U. S. A. 102:9294–9299.

Downloaded from http://jvi.asm.org/ on March 4, 2013 by NATL INST OF INFECTIOUS DISEAS

JCM
Journals.ASM.org

Japanese Reference Panel of Blood Specimens for Evaluation of Hepatitis C Virus RNA and Core Antigen Quantitative Assays

Asako Murayama,[a] Nao Sugiyama,[a] Koichi Watashi,[a] Takahiro Masaki,[a] Ryosuke Suzuki,[a] Hideki Aizaki,[a] Toshiaki Mizuochi,[b] Takaji Wakita,[a] and Takanobu Kato[a]

Department of Virology II, National Institute of Infectious Diseases, Tokyo, Japan,[a] and Department of Research on Blood and Biological Products, National Institute of Infectious Diseases, Tokyo, Japan[b]

An accurate and reliable quantitative assay for hepatitis C virus (HCV) is essential for measuring viral propagation and the efficacy of antiviral therapy. There is a growing need for domestic reference panels for evaluation of clinical assay kits because the performance of these kits may vary with region-specific genotypes or polymorphisms. In this study, we established a reference panel by selecting 80 donated blood specimens in Japan that tested positive for HCV. Using this panel, we quantified HCV viral loads using two HCV RNA kits and five core antigen (Ag) kits currently available in Japan. The data from the two HCV RNA assay kits showed excellent correlation. All RNA titers were distributed evenly across a range from 3 to 7 log IU/ml. Although the data from the five core Ag kits also correlated with RNA titers, the sensitivities of individual kits were not sufficient to quantify viral load in all samples. As calculated by the correlation with RNA titers, the theoretical lower limits of detection by these core Ag assays were higher than those for the detection of RNA. Moreover, in several samples in our panel, core Ag levels were underestimated compared to RNA titers. Sequence analysis in the HCV core region suggested that polymorphisms at amino acids 47 to 49 of the core Ag were responsible for this underestimation. The panel established in this study will be useful for estimating the quality of currently available and upcoming HCV assay kits; such quality control is essential for clinical usage of these kits.

Hepatitis C virus (HCV) is a major cause of chronic liver disease worldwide (15). There is no protective vaccine against this virus, and once an individual is infected, HCV often establishes persistent infection and leads to chronic hepatitis, cirrhosis, and hepatocellular carcinoma (9). The most widely used therapy for HCV infection is the combined administration of pegylated alpha interferon and ribavirin (29). However, this treatment is problematic, as it has limited efficacy, high cost, and severe adverse effects (8, 25). To estimate the outcome of antiviral therapy, and to understand the state of viral propagation, it is important to determine the HCV viral load in chronic hepatitis C patients by the use of accurate and reliable HCV quantitative assays (9, 14). For this purpose, several commercial assay kits for HCV RNA and core antigen (Ag) quantification are currently used in Japan. For quantification of HCV RNA levels, two real-time quantitative reverse transcription-PCR (qRT-PCR)-based assay kits are available, including the COBAS AmpliPrep/COBAS TaqMan HCV test (CAP/CTM-RNA; Roche Diagnostics, Tokyo, Japan) and the Abbott RealTime HCV test (ART-RNA; Abbott Japan, Tokyo, Japan). These assays are known to have high sensitivity and a wide dynamic range, but they require technical skill and attention to maintaining the specified conditions (4–6, 16, 24, 33–35). Alternatively, HCV viremia can be quantified by assessment of HCV core Ag level (1–3, 7, 10, 12, 13, 17–22, 27, 30–32). Five HCV core Ag assay kits are commercially available in Japan, including Architect HCV Ag (Architect-Ag; Abbott Japan), Lumipulse Ortho HCV Ag (Lumipulse-Ag; Fujirebio, Tokyo, Japan), Lumispot Eiken HCV Ag (Lumispot-Ag; Eiken Chemical, Tokyo, Japan), the Ortho HCV Ag ELISA test (ELISA-Ag; Ortho Clinical Diagnostics, Tokyo, Japan), and the Ortho HCV Ag IRMA test (IRMA-Ag; Ortho Clinical Diagnostics, Tokyo, Japan). These assays have some disadvantages compared to those measuring HCV RNA (notably, low sensitivity and narrow range of quantification) but also have some advantages (including ease of use, reduced risk of contamination, reduced cost, and reliability even with samples stored at room temperature for extended periods of time [1, 32]). Although core Ag levels are thought to be related closely to HCV RNA titers, the correlation and linearity of core Ag levels have not yet been fully evaluated. In addition, these quantitative parameters are known to be affected by nucleotide and amino acid sequences at the target regions of the assays (5, 6, 28, 34), and this sequence variation depends on genotypes or predominant strains in specific geographical regions.

In this study, we established a Japanese reference panel of samples for evaluation of HCV RNA and core Ag levels by collecting donated blood specimens that tested positive for HCV RNA and anti-HCV antibodies. Using this reference panel, we evaluated the HCV loads in these specimens with two HCV RNA assay kits and five core Ag assay kits and assessed correlations among the data generated by these kits.

MATERIALS AND METHODS

Preparation of reference panel. To establish a reference panel for HCV quantitative assays, a total of 80 donated plasma samples were selected. All of these specimens, supplied by the Japanese Red Cross Blood Centers, tested positive for the presence of HCV RNA and anti-HCV antibodies. These samples, collected in Japan from May to September of 2007, were obtained from Japanese blood donor volunteers in various regions of

Received 20 February 2012 Returned for modification 21 March 2012 Accepted 30 March 2012
Published ahead of print 11 April 2012
Address correspondence to Takanobu Kato, takato@nih.go.jp.
Supplemental material for this article may be found at http://jcm.asm.org/.
Copyright © 2012, American Society for Microbiology. All Rights Reserved.
doi:10.1128/JCM.00487-12

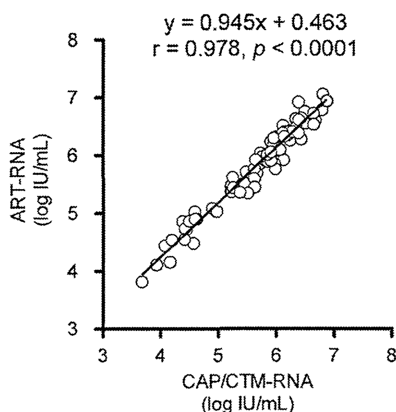

FIG 1 Correlation of HCV RNA titers as quantified by two commercial kits.

Japan. The samples were divided into 1-ml aliquots and stored at −80°C until use.

Quantification of HCV RNA and core Ag. The HCV RNA titer was measured with two real-time qRT-PCR kits, CAP/CTM-RNA (detection range, 1.5×10^1 to 6.9×10^7 IU/ml) and ART-RNA (detection range, 1.2×10^1 to 1.0×10^8 IU/ml). Additionally, samples were assessed using five HCV core Ag assay kits, including Architect-Ag (detection range, 3 to 20,000 fmol/liter), Lumipulse-Ag (detection range, 50 to 50,000 fmol/liter), Lumispot-Ag (detection range, 20 to 400,000 fmol/liter), ELISA-Ag (detection range, 44.4 to 3,600 fmol/liter), and IRMA-Ag (detection range, 20 to 20,000 fmol/liter). All assays were performed by the respective manufacturers at their research laboratories.

Sequencing and genotyping of HCV in reference panel samples. Viral RNA was extracted with the QIAamp viral RNA kit (Qiagen, Valencia, CA) from 140 μl of each plasma sample. HCV RNA was amplified by RT-PCR with primers corresponding to the 5′ untranslated region (UTR) (43S-IH, 5′-CCTGTGAGGAACTACTGTCTTC-3′; c/s17-ssp, 5′-CCGGGAGAGCCATAGTGGTCTGCG-3′) and the E1 region (1323R-IH, 5′-GGCGACCAGTTCATCATCAT-3′); the amplified products were sequenced directly. HCV genotypes of the isolated strains were assigned by phylogenetic analysis using an alignment with a representative strain of each genotype.

Statistical analysis. The correlations of obtained quantitative data were assessed by Pearson's correlation coefficient analysis, and values for *r* and *P* were calculated. A *P* value of <0.05 was considered to indicate statistical significance. Analysis was performed using Prism 5 software (GraphPad Software, Inc., La Jolla, CA).

Nucleotide sequence accession numbers. The accession numbers of C-01 to C-80 are AB705312 to AB705391, respectively.

RESULTS

Quantification of HCV RNA levels. The reference panel established in this work was used to measure HCV RNA levels with the CAP/CTM-RNA and ART-RNA kits. The correlation of the data obtained with the two kits is shown in Fig. 1. The RNA titers of these samples were distributed evenly, and all values were within the dynamic ranges of both assays. The HCV titers ranged from 3.68 to 6.88 and 3.82 to 7.08 log IU/ml in CAP/CTM-RNA and ART-RNA, respectively, and the correlation was significant ($r = 0.978$; $P < 0.0001$).

Quantification of HCV core Ag levels. HCV core Ag levels were measured using Architect-Ag, Lumipulse-Ag, Lumispot-Ag, ELISA-Ag, and IRMA-Ag kits. Among the 80 specimens in the reference panel, core Ag levels could be measured in all samples using Architect-Ag and ELISA-Ag kits, whereas core Ag levels were below the detection limit in 4, 2, and 1 samples using Lumipulse-Ag, Lumispot-Ag, and IRMA-Ag kits, respectively (Fig. 2; also, see Fig. S1 in the supplemental material). Significant correlations were observed between assays of HCV core Ag and HCV RNA ($r = 0.9065$ to 0.9666 and $P < 0.0001$ compared with CAP/CTM-RNA data [Fig. 2]); $r = 0.8877$ to 0.9552 and $P < 0.0001$ compared with ART-RNA data [see Fig. S1 in the supplemental material]). The theoretical lower limits of detection of these assays were calculated by use of these correlation formulas and were 3.2 and 3.4 log IU/ml for Architect-Ag, 4.2 and 4.2 log IU/ml for Lumipulse-Ag, 3.7 and 3.9 log IU/ml for Lumispot-Ag, 3.6 and 3.8 log IU/ml for ELISA-Ag, and 3.6 and 3.8 log IU/ml for IRMA-Ag (compared to CAP/CTM-RNA and ART-RNA, respectively). These calculated detection limits were substantially higher than those for the RNA quantitative assays (1.18 and 1.08 log IU/ml for CAP/CTM-RNA and ART-RNA, respectively).

In addition, we found that several samples showed considerable deviation from the linear regression (Fig. 2; also, see Fig. S1 in the supplemental material). To identify the deviating samples, we used Bland-Altman plot analysis (Fig. 3; also, see Fig. S2 in the supplemental material). This plot shows the difference between the titer values of HCV RNA and core Ag as a function of the average of these two values. Several samples demonstrated discordance between the measured HCV RNA and core Ag levels. Among these samples, we focused on samples with discordant results in multiple core Ag assays compared to both RNA quantitative assays. For sample C-01, core Ag levels were underestimated when measured with Architect-Ag, Lumipulse-Ag, and Lumispot-Ag in comparison with CAP/CTM-RNA (Fig. 3) and when measured with Architect-Ag, Lumipulse-Ag, Lumispot-Ag, and IRMA-Ag in comparison with ART-RNA (see Fig. S2 in the supplemental material). Likewise, for sample C-73, core Ag levels were underestimated when measured with Architect-Ag, Lumipulse-Ag, and IRMA-Ag in comparison with CAP/CTM-RNA (Fig. 3) and when measured with Architect-Ag and Lumipulse-Ag in comparison with ART-RNA (see Fig. S2 in the supplemental material). Thus, sample-specific underestimation was observed in several HCV core Ag kits.

Nucleotide sequences in core region of reference panel samples. To clarify the sources of these underestimates of HCV core Ag levels, HCV RNA was extracted from each of the samples in the reference panel, and the nucleotide sequences of core regions were determined. Phylogenetic analysis with these sequences permitted classification of the individual strains by genotype. Of 80 samples in the reference panel, 1 (1.3%) was genotype 1a, 35 (43.8%) were genotype 1b, 26 (32.5%) were genotype 2a, and 18 (22.5%) were genotype 2b (Table 1; also, see Fig. S3 in the supplemental material). These strains were distributed evenly among reference strains of each genotype and cover the sequence diversity of strains isolated in Japan (see Fig. S3 in the supplemental material). The genotypes of samples associated with underestimated core Ag values (samples C-01 and C-73) were both classified as genotype 2a.

Predicted amino acid sequences of HCV core protein were aligned with the consensus core protein sequence for the genotype 1b strains obtained in this study (see Fig. S4 in the supplemental material). Excluding the genotype-specific sequence variations, a specific amino acid polymorphism was identified at amino acid (aa) residue 48 (Ala to Thr) in samples C-01 and C-73. Sample C-01, which yielded underestimated values in most core Ag assays, also possessed an additional polymorphism in the same region,

Downloaded from http://jcm.asm.org/ on May 17, 2012 by NATL INST OF INFECTIOUS DISEAS

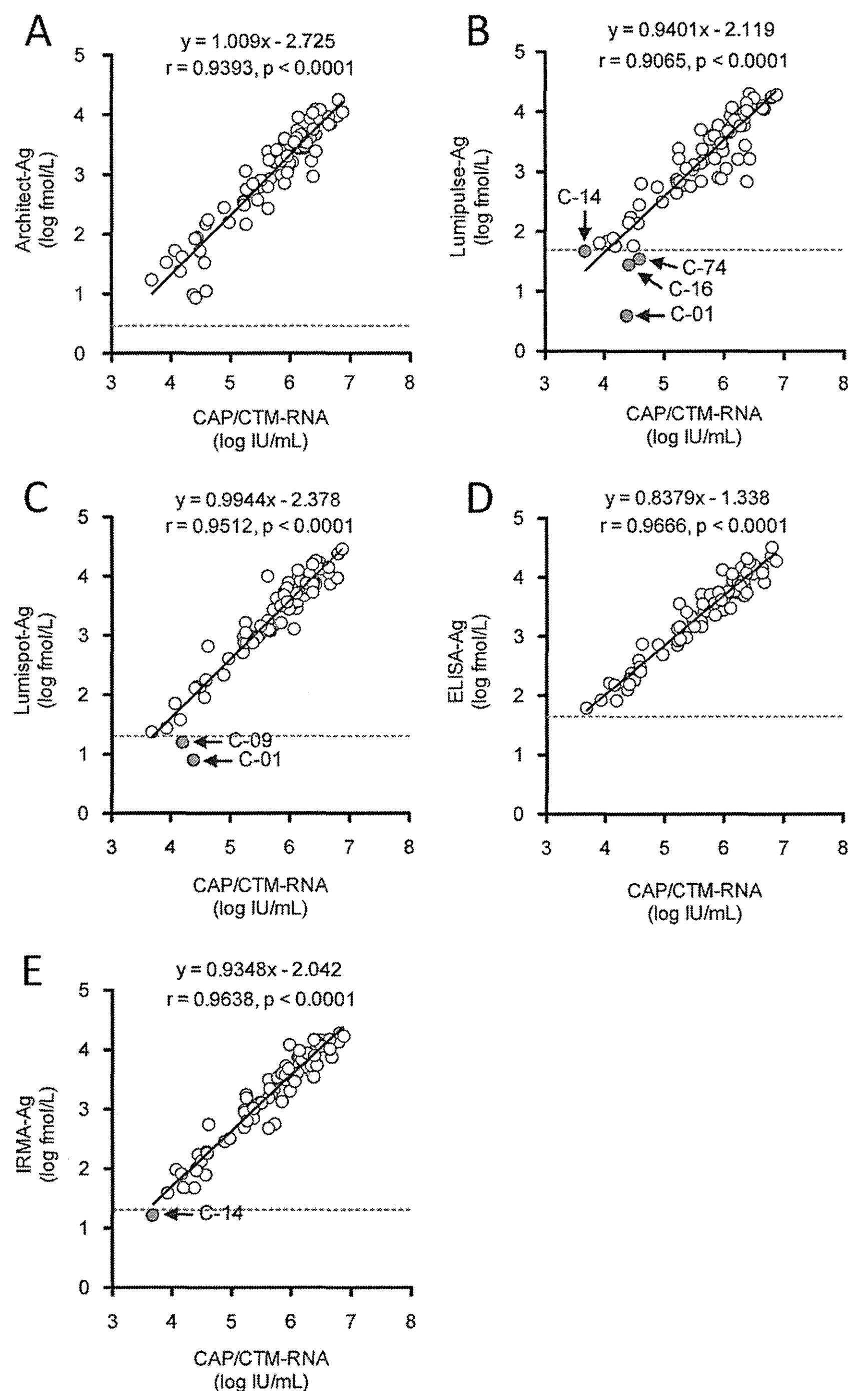

FIG 2 Correlation between CAP/CTM-RNA and core Ag levels as quantified by five commercial kits. Data for core Ag levels were converted to log fmol/liter prior to analysis. In each plot, the lower limit of detection of the respective core Ag assay is indicated by a dotted line. Data for samples below the lower detection limit of each assay are indicated by shaded circles labeled with the respective sample designations.

specifically an Arg-to-Gly substitution at aa 47. We suspected that these polymorphisms altered the antigenicity of the core protein, thereby reducing detected core Ag levels and leading to underestimation of values by the core Ag quantification kits. To assess the correlation of these polymorphisms with the underestimation of core Ag values, strains containing polymorphisms in this region (at aa 47 to 49 [Fig. 4]) were identified in Bland-Altman plots of HCV RNA and core Ag (Fig. 3; also, see Fig. S2 in the supplemental material). A total of 12 strains exhibited polymorphisms at these positions, including 2 strains of genotype 1b, 8 of genotype 2a, and 2 of genotype 2b (Table 1). In the Bland-Altman plot of CAP/CTM-RNA and Architect-Ag, 4 of 12 values (for samples C-01, C-16, C-73, and C-74) were located under the line of the lower 95% limit of agreement (Fig. 3A). Likewise, in the plot of CAP/CTM-RNA and Lumipulse-Ag, 3 of 12 values (those for samples C-01, C-67, and C-73) were located under the line of the lower

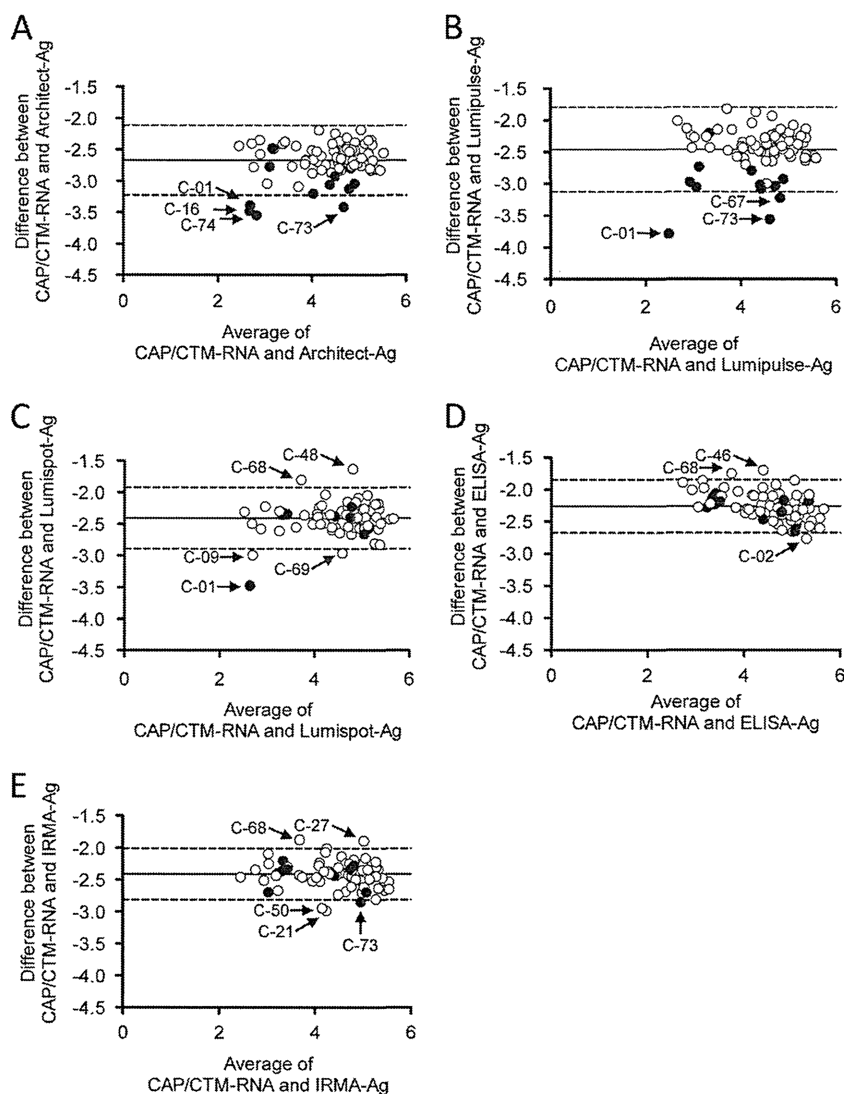

FIG 3 Bland-Altman plot analysis of CAP/CTM-RNA and core Ag levels as quantified by five commercial kits. These plots show the difference between the values of HCV RNA and core Ag as a function of the average of these two values. Data for core Ag levels were converted to log fmol/liter prior to analysis. The bias and 95% limits of agreements are indicated by solid and dashed lines, respectively. Data for samples with polymorphisms at amino acid residues 47 to 49 are indicated by solid circles. Data points outside the 95% limits are indicated by arrows labeled with the sample designations.

95% limit of agreement (Fig. 3B). In these plots, underestimation for samples that lacked these polymorphisms (at aa 47 to 49) was not detected. In the plot of CAP/CTM-RNA and Lumispot-Ag, only 1 sample (C-01) was located under the line of the lower 95% limit of agreement, but this sample exhibited the most discordant value (Fig. 3C). In the plot of CAP/CTM-RNA and ELISA-Ag, no correlation between polymorphisms at these positions and underestimation was observed (Fig. 3D). In the plot of CAP/CTM-RNA and IRMA-Ag, sample C-73 was located under the line of the lower 95% limit of agreement, as were other samples that lacked polymorphisms at aa 47 to 49 (Fig. 3E). Similar trends were observed in comparison with ART-RNA levels (see Fig. S2 in the supplemental material). Based on these results, the levels of HCV core Ag measured with Architect-Ag and Lumipulse-Ag seem to be more strongly affected by single polymorphisms at these positions. In the case of Lumispot-Ag, underestimation may be limited to specimens with multiple polymorphisms at these positions.

TABLE 1 Number of reference panel strains with polymorphisms at amino acid residues 47 to 49 of the HCV core region

	No. (%) of strains	
Genotype	Total	With polymorphisms
1a	1	0
1b	35	2 (5.7)
2a	26	8 (30.8)
2b	18	2 (11.8)
Total	80	12 (15.0)

DISCUSSION

The quantification of HCV viral load is essential for selecting an appropriate antiviral strategy and for monitoring the efficacy of treatment. Since HCV is known to be highly variable and rapidly

Downloaded from http://jcm.asm.org/ on May 17, 2012 by NATL INST OF INFECTIOUS DISEAS

```
aa          1                                                        60
1b-cons.    MSTNPKPQRKTKRNTNRRPQDVKFPGGGQIVGGVYLLPRRGPRLGVRATRKTSERSQPRG
C-16(1b)    ................................................P...........
C-53(1b)    ................................................P...........
C-01(2a)    ..............................................GT............
C-03(2a)    ...............L...............................T............
C-12(2a)    ...T...........................................T............
C-65(2a)    ...T............................................A...........
C-67(2a)    ...............................................T............
C-71(2a)    ...............................................T............
C-73(2a)    ...............................................T............
C-76(2a)    ................................................A...........
C-08(2b)    ................................................P...........
C-74(2b)    ................................................P...........
```

FIG 4 Alignment of the first 60 amino acids of the HCV core region of strains with polymorphisms at amino acid residues 47 to 49. The position numbers are given at the top. Dots indicate identical amino acids. The consensus sequence of 1b strains (1b cons.) isolated in this study was determined and used as a reference sequence. Genotypes of strains are given in parentheses. Positions of polymorphisms are indicated by inverted triangles above the sequence alignment.

evolving (23, 26), the assays for quantifying this virus should be unaffected by sequence polymorphisms. In this study, we established a reference panel with HCV-positive samples and evaluated the correlation among multiple assays for HCV RNA and core Ag quantification.

Using this reference panel, we found that the results from two HCV RNA assay kits, CAP/CTM-RNA and ART-RNA, correlated with excellent agreement ($r = 0.978$, $P < 0.0001$ [Fig. 1]), although discrepancies for values generated by these two assays have been reported for strains of genotypes 1, 2, and 4 (5, 6, 34). In Japan, the prevalent genotypes are 1b, 2a, and 2b (11); no genotype 4 sample was included in our reference panel (Table 1). In quantification with CAP/CTM-RNA, underestimation of HCV RNA titer has been reported for French genotype 2 samples (5). In our panel, no underestimation was observed for data from genotype 2 samples compared to values obtained using ART-RNA. Therefore, underestimation in quantification with CAP/CTM-RNA is expected to be rare in Japanese samples, and the two assays for HCV RNA quantification should be considered accurate and reliable, at least for Japanese samples. Additionally, the prepared reference panel appears to be suitable for the evaluation of HCV quantification assays, because genotypes of samples in this panel are representative of those found in Japan and viral loads are distributed evenly across the range of expected titers.

The quantification of HCV core Ag is an alternative test for HCV infection and viral load. However, in this study, several core Ag quantitative assays failed to provide accurate results for all of the samples in the reference panel (Fig. 2). Some quantified values were below the kits' detection limits. This shortcoming was mainly attributable to the lower sensitivity of the core Ag assay kits; increased sensitivity is urged in the future development of HCV core Ag kits. Among the kits tested here, Architect-Ag assay exhibited the highest sensitivity and was sufficient for quantifying the viral load in all samples. However, even in the case of Architect-Ag, theoretical lower limits of detection, calculated by correlation formula using CAP/CTM-RNA and ART-RNA, were 3.2 and 3.4 log IU/ml, respectively; these detection limits still exceeded the lower limits of the HCV RNA quantification assays. Therefore, the sensitivity of the available HCV core Ag assays is still insufficient to detect low-titer HCV infections. Core Ag kits therefore may be unsuitable for the detection of breakthrough hepatitis during antiviral therapy or for the detection of HCV infection in a window period.

Comparison between HCV RNA and core Ag assays revealed good correlations, with r coefficients ranging from 0.8877 to 0.9666 and P values being less than 0.0001 (Fig. 2; also, see Fig. S1 in the supplemental material). Therefore, the HCV core Ag levels may serve as an alternative to HCV RNA levels when titers remain within the detection ranges of the core Ag kits. However, several discordances were detected when core Ag levels were compared with those of HCV RNA. For one sample in our panel (sample C-01), core Ag levels were lower than expected when quantified using any of the three core Ag kits (Architect-Ag, Lumipulse-Ag, and Lumispot-Ag) (Fig. 3; also, see Fig. S2 in the supplemental material). Another sample (C-73) also yielded lower-than-expected levels when assayed with Architect-Ag and Lumipulse-Ag kits. Sequence analysis of the core region revealed that polymorphisms at aa 47 and 48 correlated with these underestimates by core Ag kits (see Fig. S4 in the supplemental material). These results are consistent with our previous study, which suggested that core Ag levels of HCV strain JFH-1 were underestimated by the Lumipulse-Ag kit in comparison to the ELISA-Ag assay (28). Strain JFH-1 harbors an Ala-to-Thr substitution at aa 48; conversion of Thr to Ala at this position in JFH-1 was sufficient to overcome this underestimation. This region of the core Ag presumably corresponds to one of the epitopes recognized by the monoclonal antibodies used in the Lumipulse-Ag kit, such that polymorphisms at this position affected the antigenicity of the core protein. In this study, we found that the presence of other polymorphisms in this region (aa 47 to 49) correlated with reduced core Ag levels as detected by Lumipulse-Ag, as well as by other assays (Architect-Ag and Lumispot-Ag). Sample C-01 demonstrated a drastic deviation from expected core Ag levels in these assays (Fig. 3; also, see Fig. S2 in the supplemental material). The HCV strain in this sample contains two polymorphisms (Arg to Gly at aa 47 and Ala to Thr at aa 48); the multiple polymorphisms may impair antibody binding more severely and therefore result in underestimation of core Ag levels. Interestingly, this sample exhibited reasonable core Ag levels when assayed using ELISA-Ag. Thus, the underestimation of core protein levels in this sample was kit dependent, suggesting the targeting of distinct epitopes by the antibodies used in each of these kits. This hypothesis could not be confirmed, because the identity of the epitopes targeted by each kit is proprietary.

Of 12 samples with amino acid polymorphisms in this region, 2 (5.7%) were of genotype 1b, 8 (30.8%) were of genotype 2a, and

TABLE 2 Number of strains in the sequence database[a] with polymorphisms at amino acid residues 47 to 49 of the HCV core region

	No. (%) of strains				
		With polymorphism			
Genotype	Tested	At aa 47 (R/C, G)	At aa 48 (A/T, P)	At aa 49 (T/A, P, L)	Total
1b	543	2 (0.36)	4 (0.74)	16 (2.96)	22 (4.1)
2a	24	0	6 (25.0)	1 (4.2)	7 (29.2)
2b	39	0	0	2 (6.9)	2 (6.9)

[a] http://s2as02.genes.nig.ac.jp/.

2 (11.8%) were of genotype 2b (Table 1). Searches of the Hepatitis Virus Database (http://s2as02.genes.nig.ac.jp/) revealed that corresponding amino acid polymorphisms were observed in 22 of 543 strains (4.1%) of genotype 1b, 7 of 24 strains (29.2%) of genotype 2a, and 2 of 39 strains (6.9%) of genotype 2b (Table 2). These percentages were consistent with our observations in the proposed reference panel. These data (our results and those from the database) clearly indicate that genotype 2a strains are the most frequent source of underestimation of core Ag levels. Notably, our search of the sequence database did not yield any HCV strain with multiple polymorphisms in the region from aa 47 to 49, as we saw in our sample C-01. Therefore, strains with such multiple polymorphisms are rare so far, but detection of this isolate among donated blood specimens suggests that such HCV strains could be emerging in clinical samples. For patients harboring such strains, HCV viral load may be underestimated if measurement of HCV viral load is performed by core Ag assay. Such underestimates may result in erroneous selection of therapy, adversely affecting patient outcome. Thus, this shortcoming in HCV core Ag assay kits needs to be addressed.

There is a growing need for evaluation of clinical assay kits with domestic specimen reference panels, since the performance of these kits may be affected by the genotypes or polymorphisms of predominant strains in different geographic regions. To our knowledge, such an investigation of HCV clinical assay kits with domestic specimens has not previously been conducted in Japan. The Japanese HCV reference panel described here was generated with plasma samples collected from Japanese volunteers. Each sample was divided into small aliquots, and the panel was prepared in multiple sets. The samples in our HCV reference panel represent the predominant strains and genotypes seen in Japan. We expect that this reference panel will be of use for the development, evaluation, and optimization of HCV assay kits for the Japanese clinical market.

In conclusion, we have established a Japanese reference panel for evaluation of HCV quantification assays. Using this reference panel, we found that two assay kits for HCV RNA could quantify HCV titers concordantly. We also found that the data generated by HCV core Ag assay kits correlated with the results of HCV RNA assays. However, the nominal core Ag levels measured by several kits underestimated actual levels for HCV samples with polymorphisms at aa 47 to 49 of the core Ag. The panel established in this study is expected to be useful for estimating the accuracy of currently available and upcoming HCV assay kits; such quality control is essential for clinical usage of these kits.

ACKNOWLEDGMENTS

This work was performed as part of a project for the preparation of reference panels of infectious disease specimens at the National Institute of Infectious Diseases in Japan. This work was also partly supported by grants-in-aid from the Japan Society for the Promotion of Science; the Ministry of Health, Labor and Welfare of Japan; the Ministry of Education, Culture, Sports, Science and Technology; and the Research on Health Sciences Focusing on Drug Innovation from the Japan Health Sciences Foundation.

We are grateful to Shun-ya Momose, Shigeharu Uchida, and Satoru Hino (Blood Service Headquarters, Japanese Red Cross Society) for providing specimens, to Tetsuro Suzuki (Department of Infectious Diseases, Hamamatsu University School of Medicine) for contribution to establish the reference panel, and to Kazuo Kobayashi and Masashi Tatsumi (the Committee of the Reference Panels of Infectious Disease Specimens at the National Institute of Infectious Diseases in Japan) for their helpful suggestions. We also thank the manufacturers of HCV quantification kits, including Roche Diagnostics (Tokyo, Japan), Abbott Japan (Tokyo, Japan), Fujirebio (Tokyo, Japan), Eiken Chemical (Tokyo, Japan), and Ortho Clinical Diagnostics (Tokyo, Japan), for quantification of reference panel samples.

REFERENCES

1. **Alvarez M, Planelles D, Vila E, Montoro J, Franco E.** 2004. Prolonged hepatitis C virus seroconversion in a blood donor, detected by HCV antigen test in parallel with HCV RNA. Vox Sang. **86**:266–267.
2. **Aoyagi K, et al.** 1999. Development of a simple and highly sensitive enzyme immunoassay for hepatitis C virus core antigen. J. Clin. Microbiol. 37:1802–1808.
3. **Aoyagi K, et al.** 2001. Performance of a conventional enzyme immunoassay for hepatitis C virus core antigen in the early phases of hepatitis C infection. Clin. Lab. **47**:119–127.
4. **Bossler A, et al.** 2011. Performance of the COBAS(R) AmpliPrep/COBAS TaqMan(R) automated system for hepatitis C virus (HCV) quantification in a multi-center comparison. J. Clin. Virol. **50**:100–103.
5. **Chevaliez S, Bouvier-Alias M, Brillet R, Pawlotsky JM.** 2007. Overestimation and underestimation of hepatitis C virus RNA levels in a widely used real-time polymerase chain reaction-based method. Hepatology **46**: 22–31.
6. **Elkady A, et al.** 2010. Performance of two real-time RT-PCR assays for quantitation of hepatitis C virus RNA: evaluation on HCV genotypes 1–4. J. Med. Virol. 82:1878–1888.
7. **Enomoto M, et al.** 2005. Chemiluminescence enzyme immunoassay for monitoring hepatitis C virus core protein during interferon-alpha2b and ribavirin therapy in patients with genotype 1 and high viral loads. J. Med. Virol. 77:77–82.
8. **Feld JJ, Hoofnagle JH.** 2005. Mechanism of action of interferon and ribavirin in treatment of hepatitis C. Nature **436**:967–972.
9. **Feld JJ, Liang TJ.** 2006. Hepatitis C—identifying patients with progressive liver injury. Hepatology 43:S194–S206.
10. **Icardi G, et al.** 2001. Novel approach to reduce the hepatitis C virus (HCV) window period: clinical evaluation of a new enzyme-linked immunosorbent assay for HCV core antigen. J. Clin. Microbiol. **39**:3110–3114.
11. **Ikeda K, et al.** 1996. Hepatitis C virus subtype 3b infection in a hospital in Japan: epidemiological study. J. Gastroenterol. **31**:801–805.
12. **Kaiser T, et al.** 2008. Kinetics of hepatitis C viral RNA and HCV-antigen during dialysis sessions: evidence for differential viral load reduction on dialysis. J. Med. Virol. **80**:1195–1201.
13. **Leary TP, et al.** 2006. A chemiluminescent, magnetic particle-based immunoassay for the detection of hepatitis C virus core antigen in human serum or plasma. J. Med. Virol. **78**:1436–1440.
14. **Liang TJ.** 1998. Combination therapy for hepatitis C infection. N. Engl. J. Med. 339:1549–1550.
15. **Liang TJ, Rehermann B, Seeff LB, Hoofnagle JH.** 2000. Pathogenesis, natural history, treatment, and prevention of hepatitis C. Ann. Intern. Med. 132:296–305.
16. **Matsuura K, et al.** 2009. Abbott RealTime hepatitis C virus (HCV) and Roche Cobas AmpliPrep/Cobas TaqMan HCV assays for prediction of sustained virological response to pegylated interferon and ribavirin in chronic hepatitis C patients. J. Clin. Microbiol. 47:385–389.

Downloaded from http://jcm.asm.org/ on May 17, 2012 by NATL INST OF INFECTIOUS DISEAS

17. **Mederacke I, et al.** 2009. Performance and clinical utility of a novel fully automated quantitative HCV-core antigen assay. J. Clin. Virol. **46**:210–215.
18. **Medici MC, et al.** 2011. Hepatitis C virus core antigen: analytical performances, correlation with viremia and potential applications of a quantitative, automated immunoassay. J. Clin. Virol. **51**:264–269.
19. **Miedouge M, et al.** 2010. Analytical evaluation of HCV core antigen and interest for HCV screening in haemodialysis patients. J. Clin. Virol. **48**: 18–21.
20. **Morota K, et al.** 2009. A new sensitive and automated chemiluminescent microparticle immunoassay for quantitative determination of hepatitis C virus core antigen. J. Virol. Methods **157**:8–14.
21. **Moscato GA, et al.** 2011. Quantitative determination of hepatitis C core antigen in therapy monitoring for chronic hepatitis C. Intervirology **54**: 61–65.
22. **Nubling CM, Unger G, Chudy M, Raia S, Lower J.** 2002. Sensitivity of HCV core antigen and HCV RNA detection in the early infection phase. Transfusion **42**:1037–1045.
23. **Ogata N, Alter HJ, Miller RH, Purcell RH.** 1991. Nucleotide sequence and mutation rate of the H strain of hepatitis C virus. Proc. Natl. Acad. Sci. U. S. A. **88**:3392–3396.
24. **Park Y, Lee JH, Kim BS, Kim DY, Han KH, Kim HS.** 2010. New automated hepatitis C virus (HCV) core antigen assay as an alternative to real-time PCR for HCV RNA quantification. J. Clin. Microbiol. **48**:2253–2256.
25. **Pawlotsky JM.** 2006. Therapy of hepatitis C: from empiricism to eradication. Hepatology **43**:S207–S220.
26. **Robertson B, et al.** 1998. Classification, nomenclature, and database development for hepatitis C virus (HCV) and related viruses: proposals for standardization. Arch. Virol. **143**:2493–2503.
27. **Ross RS, et al.** 2010. Analytical performance characteristics and clinical utility of a novel assay for total hepatitis C virus core antigen quantification. J. Clin. Microbiol. **48**:1161–1168.
28. **Saeed M, et al.** 2009. Evaluation of hepatitis C virus core antigen assays in detecting recombinant viral antigens of various genotypes. J. Clin. Microbiol. **47**:4141–4143.
29. **Seeff LB, Hoofnagle JH.** 2002. National Institutes of Health Consensus Development Conference: management of hepatitis C: 2002. Hepatology **36**:S1–S2.
30. **Takahashi M, Saito H, Higashimoto M, Atsukawa K, Ishii H.** 2005. Benefit of hepatitis C virus core antigen assay in prediction of therapeutic response to interferon and ribavirin combination therapy. J. Clin. Microbiol. **43**:186–191.
31. **Tanaka E, et al.** 2000. Evaluation of a new enzyme immunoassay for hepatitis C virus (HCV) core antigen with clinical sensitivity approximating that of genomic amplification of HCV RNA. Hepatology **32**:388–393.
32. **Tanaka Y, et al.** 2003. High stability of enzyme immunoassay for hepatitis C virus core antigen-evaluation before and after incubation at room temperature. Hepatol. Res. **26**:261–267.
33. **Vermehren J, et al.** 2008. Differences between two real-time PCR-based hepatitis C virus (HCV) assays (RealTime HCV and Cobas AmpliPrep/Cobas TaqMan) and one signal amplification assay (Versant HCV RNA 3.0) for RNA detection and quantification. J. Clin. Microbiol. **46**:3880–3891.
34. **Vermehren J, et al.** 2011. Development of a second version of the Cobas AmpliPrep/Cobas TaqMan hepatitis C virus quantitative test with improved genotype inclusivity. J. Clin. Microbiol. **49**:3309–3315.
35. **Vermehren J, et al.** 2011. Multi-center evaluation of the Abbott RealTime HCV assay for monitoring patients undergoing antiviral therapy for chronic hepatitis C. J. Clin. Virol. **52**:133–137.

Visualization and Measurement of ATP Levels in Living Cells Replicating Hepatitis C Virus Genome RNA

Tomomi Ando[1,2], Hiromi Imamura[3], Ryosuke Suzuki[1], Hideki Aizaki[1], Toshiki Watanabe[2], Takaji Wakita[1], Tetsuro Suzuki[4]*

1 Department of Virology II, National Institute of Infectious Diseases, Tokyo, Japan, 2 Graduate School of Frontier Sciences, The University of Tokyo, Tokyo, Japan, 3 The Hakubi Center and Graduate School of Biostudies, Kyoto University, Kyoto, Japan, 4 Hamamatsu University School of Medicine, Department of Infectious Diseases, Hamamatsu, Japan

Abstract

Adenosine 5′-triphosphate (ATP) is the primary energy currency of all living organisms and participates in a variety of cellular processes. Although ATP requirements during viral lifecycles have been examined in a number of studies, a method by which ATP production can be monitored in real-time, and by which ATP can be quantified in individual cells and subcellular compartments, is lacking, thereby hindering studies aimed at elucidating the precise mechanisms by which viral replication energized by ATP is controlled. In this study, we investigated the fluctuation and distribution of ATP in cells during RNA replication of the hepatitis C virus (HCV), a member of the *Flaviviridae* family. We demonstrated that cells involved in viral RNA replication actively consumed ATP, thereby reducing cytoplasmic ATP levels. Subsequently, a method to measure ATP levels at putative subcellular sites of HCV RNA replication in living cells was developed by introducing a recently-established Förster resonance energy transfer (FRET)-based ATP indicator, called ATeam, into the NS5A coding region of the HCV replicon. Using this method, we were able to observe the formation of ATP-enriched dot-like structures, which co-localize with non-structural viral proteins, within the cytoplasm of HCV-replicating cells but not in non-replicating cells. The obtained FRET signals allowed us to estimate ATP concentrations within HCV replicating cells as ~5 mM at possible replicating sites and ~1 mM at peripheral sites that did not appear to be involved in HCV replication. In contrast, cytoplasmic ATP levels in non-replicating Huh-7 cells were estimated as ~2 mM. To our knowledge, this is the first study to demonstrate changes in ATP concentration within cells during replication of the HCV genome and increased ATP levels at distinct sites within replicating cells. ATeam may be a powerful tool for the study of energy metabolism during replication of the viral genome.

Citation: Ando T, Imamura H, Suzuki R, Aizaki H, Watanabe T, et al. (2012) Visualization and Measurement of ATP Levels in Living Cells Replicating Hepatitis C Virus Genome RNA. PLoS Pathog 8(3): e1002561. doi:10.1371/journal.ppat.1002561

Editor: Andrea Gamarnik, Fundación Instituto Leloir-CONICET, Argentina

Received August 22, 2011; **Accepted** January 18, 2012; **Published** March 1, 2012

Copyright: © 2012 Ando et al. This is an open-access article distributed under the terms of the Creative Commons Attribution License, which permits unrestricted use, distribution, and reproduction in any medium, provided the original author and source are credited.

Funding: This work was supported by a grant-in-aid for Scientific Research from the Japan Society for the Promotion of Science, from the Ministry of Health, Labour and Welfare of Japan and from the Ministry of Education, Culture, Sports, Science and Technology of Japan. T.A. is a research fellow of the Japan Society for the Promotion of Science. The funders had no role in study design, data collection and analysis, decision to publish, or preparation of the manuscript.

Competing Interests: The authors have declared that no competing interests exist.

* E-mail: tesuzuki@hama-med.ac.jp

Introduction

Adenosine 5′-triphosphate (ATP) is the major energy currency of cells and is involved in a variety of cellular processes, including the virus life cycle, in which ATP-dependent reactions essential for virus multiplication are catalyzed by viral-encoded enzymes or complexes consisting of viral and host-cell proteins [1]. However, the lack of a real-time monitoring system for ATP has hindered studies aimed at elucidating the mechanisms by which cellular processes are controlled through ATP. A method for measuring ATP levels in individual living cells has recently been developed using a genetically-encoded FRET-based indicator for ATP, called ATeam, which employs the epsilon subunit of a bacterial F_0F_1-ATPase [2]. The epsilon subunit has several theoretical advantages for use as an ATP indicator; i) small size (14 kDa), ii) high specific binding to ATP, iii) ATP binding induces a global conformational change and iv) ATP hydrolysis does not occur following binding [3–5]. The affinity of ATeam for ATP can be adjusted by changing various amino acid residues in the ATP-binding domain within the subunit. ATeam has enabled researchers to examine the subcellular compartmentation of ATP as well as time-dependent changes in cellular ATP levels under various physiological conditions. For example, the ATeam-based method has been used to demonstrate that ATP levels within the mitochondrial matrix are lower than those in the cytoplasm and the nucleus [2].

Hepatitis C virus (HCV) infects 2–3% of the world population and is a major cause of chronic hepatitis, liver cirrhosis and hepatocellular carcinoma [6–8]. HCV possesses a positive-strand RNA genome and belongs to the family *Flaviviridae*. A precursor polyprotein of ~3000 amino acids is post- or co-translationally processed by both viral and host proteases into at least ten viral products. The nonstructural (NS) proteins NS3, NS4A, NS4B, NS5A and NS5B are necessary and sufficient for autonomous HCV RNA replication. These proteins form a membrane-associated replication complex (RC), in which NS5B is the RNA-dependent RNA polymerase (RdRp) responsible for copying the RNA genome of the virus during replication [9,10]. NS3, in addition to its protease activity, functions as a viral helicase capable of separating duplex RNA and DNA in reactions fuelled

Author Summary

ATP is the major energy currency of living cells. Replication of the virus genome is a physiological mechanism that is known to require energy for operations such as the synthesis of DNA or RNA and their unwinding. However, it has been difficult to comprehend how the ATP level is regulated inside single living cells where the virus replicates, since average ATP values in cell extracts have only been estimated using existing methods for ATP measurement. ATeam, which was established in 2009, is a genetically-encoded Förster resonance energy transfer (FRET)-based indicator for ATP that is composed of a small bacterial protein that specifically binds ATP sandwiched between two fluorescent proteins. In this study, by applying ATeam to the subgenomic replicon system, we have developed a method to monitor ATP at putative subcellular sites of RNA replication of the hepatitis C virus (HCV), a major human pathogen associated with liver disease, in living cells. We show here, for the first time, changes in ATP concentrations at distinct sites within cells undergoing HCV RNA replication. ATeam might open the door to understanding how regulation of ATP can affect the lifecycles of pathogens.

by ATP hydrolysis [11,12]. Consistent with other positive-strand RNA viruses, replication of HCV genomic RNA is believed to occur in membrane-bound vesicles. NS3-NS5B proteins, together with several host-cell proteins, form a membrane-associated RC. The HCV RC is localized to distinct dot-like structures within the cytoplasm of HCV replicating cells and can be detected in detergent-resistant membrane structures [13].

In this study, we first used capillary electrophoresis-time-of-flight mass spectrometry (CE-TOF MS) and the original ATeam method to determine ATP levels in cells infected with HCV or replicating HCV RNA. Using these methods, together with an ATP consumption assay, we demonstrated that ATP is actively consumed in cells in which viral RNA replicates, leading to a reduction in cytoplasmic ATP compared to parental cells. To further understand the fluctuation and distribution of ATP in HCV replicating cells, we developed a system to monitor ATP at putative subcellular sites of HCV RNA replication in single living cells by applying ATeam technology to the subgenomic replicon system. Our results show that, in viral RNA-replicating cells, ATP levels are elevated at distinct dot-like structures that may play a supportive role in HCV RNA replication, while cytoplasmic levels of ATP decrease.

Results

The concentration of ATP is reduced in HCV-infected cells

As a first approach, the concentration of adenosine nucleotides within HCV-infected and non-infected cells was quantified by CE-TOF MS analysis. ATP levels were approximately 7- and 50-fold higher, respectively, than the levels of ADP and AMP in non-infected Huh-7 cells (Figure 1A). At 9 days post-infection with HCV particles produced from a wild-type JFH-1 isolate [14], the intracellular levels of ATP, ADP and AMP were significantly (52–59%) lower than those in naïve Huh-7 cells (Figure 1A). ATP/ADP and ATP/AMP ratios were comparable among HCV-infected and non-infected cells (Figure 1B). A similar result was obtained using JFH-1/4-5 cells that harbor a HCV subgenomic replicon (SGR) RNA derived from the JFH-1 isolate [15]; the intracellular ATP level of JFH-1/4-5 cells was lower than that of parental Huh-7 cells (Figure S1). These findings are basically consistent with a recent report that phosphorylation-mediated activation of AMP-activated protein kinase is inhibited in cells undergoing HCV genome replication, and that ATP/ADP ratios are similar among cells that do and do not demonstrate HCV replication [16,17].

Measurement of ATP levels in HCV-replicating cells using ATeam

To visualize ATP levels in living cells undergoing HCV genomic replication, one of the ATeam indicators, AT1.03^{YEMK}, which has a high affinity for ATP, was introduced into HCV replicon cells carrying SGR RNA or into parental Huh-7 cells and was imaged using confocal fluorescence microscopy. Consistent with previous observations in HeLa cells [2], this ATP indicator was distributed throughout the cytoplasm. FRET signals (Venus/

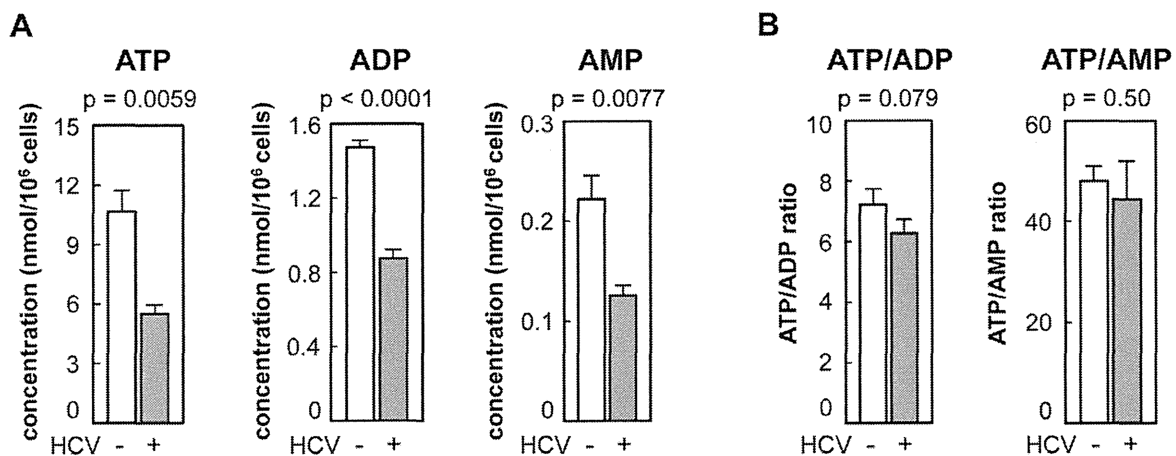

Figure 1. Levels of adenosine nucleotides in HCV-infected and non-infected Huh-7 cells determined by CE-TOF MS. (A) ATP levels were reduced in HCV-infected cells. ATP, ADP, and AMP metabolites in Huh-7 cells with (gray bars) and without (open bars) HCV infection were measured by CE-TOFMS. (B) Ratios of ATP/ADP and ATP/AMP were calculated from the results depicted in (A). All data are presented as means and standard deviation (SD) values for three independent samples. Statistical differences between HCV-infected and non-infected cells were evaluated using Student's *t*-test.

doi:10.1371/journal.ppat.1002561.g001

CFP fluorescence emission ratios), which reflect ATP levels in living cells, were calculated from the fluorescent images of CFP and Venus, a variant of YFP that is resistant to intracellular pH [18], within the cytoplasm of individual cells. Each independent measurement was plotted as indicated in Figure 2. Uniform Venus/CFP ratios were observed in Huh-7 cells. These ratios were reduced dramatically following combined treatment with 2-deoxyglucose (2DG) and Oligomycin A (OliA), which inhibit glycolysis and the oxidative phosphorylation of ADP to ATP, respectively [2]. When AT1.03$^{\mathrm{YEMK}}$ was expressed in the HCV replicon-harboring cells JFH-1/4-1, JFH-1/4-5 (genotype 2a) and NK5.1/0-9 (genotype 1b) [15], Venus/CFP ratios were significantly lower than those seen in parental Huh-7 cells. This result is consistent with the mass spectrometry results shown in Figures 1A and S1. Venus/CFP ratios were more variable in the replicon-carrying cells compared to Huh-7 cells. It is possible that ATP levels in the replicon cells correlate with viral replication levels, which may vary among the cells tested.

The consumption of ATP is increased in HCV-replicating cells

It has been reported that ATP is involved in different steps in the course of HCV replication such as in the initiation of RNA synthesis by NS5B RdRp [9]. NS3 unwinds RNA in an ATP-dependent manner and may be involved in viral replication [11,19,20]. NS4A has been shown to enhance the ability of the NS3 helicase to bind RNA in the presence of ATP [21]. In addition, ATP is generally used as a material in RNA synthesis. Together with the above results (Figures 1 and 2), one may hypothesize that active consumption of ATP in cells where HCV RNA replicates efficiently results in lower levels of cytoplasmic ATP compared to cells in the absence of the viral RNA. To study the influence of HCV RNA replication on the consumption of ATP in cells, we used permeabilized HCV replicon cells [13,22].

Following the addition of ATP to permeabilized cells, reduced ATP levels were detected using a luciferase-based assay (see Materials and Methods for details). Fifteen minutes after the addition of ATP, ATP levels in permeabilized replicon-carrying cells (JFH-1/4-1, JFH-1/4-5 and NK5.1/0-9) were reduced by 82–95%, and this reduction was greater than that observed in control Huh-7 cells (47%)(Figure 3). When the replication of HCV RNA was inhibited by pre-treatment of the cells with the cytidine analogue inhibitor of HCV NS5B polymerase, PSI-6130 [23,24], for 3 days, the reduction in ATP levels in the replicon cells was comparable to that of Huh-7 cells. A decrease in ATP reduction in the replicon cells was observed even following a 15-min treatment with the inhibitor. An effect of inhibition of viral replication on cytoplasmic ATP levels in replicon cells was also observed by ATeam-based analysis of Venus/CFP ratios following inhibition of replication by IFN-alpha (Figure S2). These results suggest that ATP is actively consumed during viral replication in HCV replicon cells, leading to decreased levels of ATP in the cytoplasm.

Development of a system to monitor ATP levels at putative subcellular sites of HCV replication in single living cells

Moradpour et al. have established functional HCV replicons that have either an epitope tag or the coding sequence for a green fluorescent protein (GFP) inserted in frame close to the C-terminus of NS5A, which they used to demonstrate incorporation of the NS5A-GFP fusion protein into the viral RC [25]. To further investigate intracellular changes in ATP during HCV replication, we generated HCV JFH-1-based subgenomic replicons harboring an ATeam insertion in the 3′ region of NS5A (SGR-ATeam), as

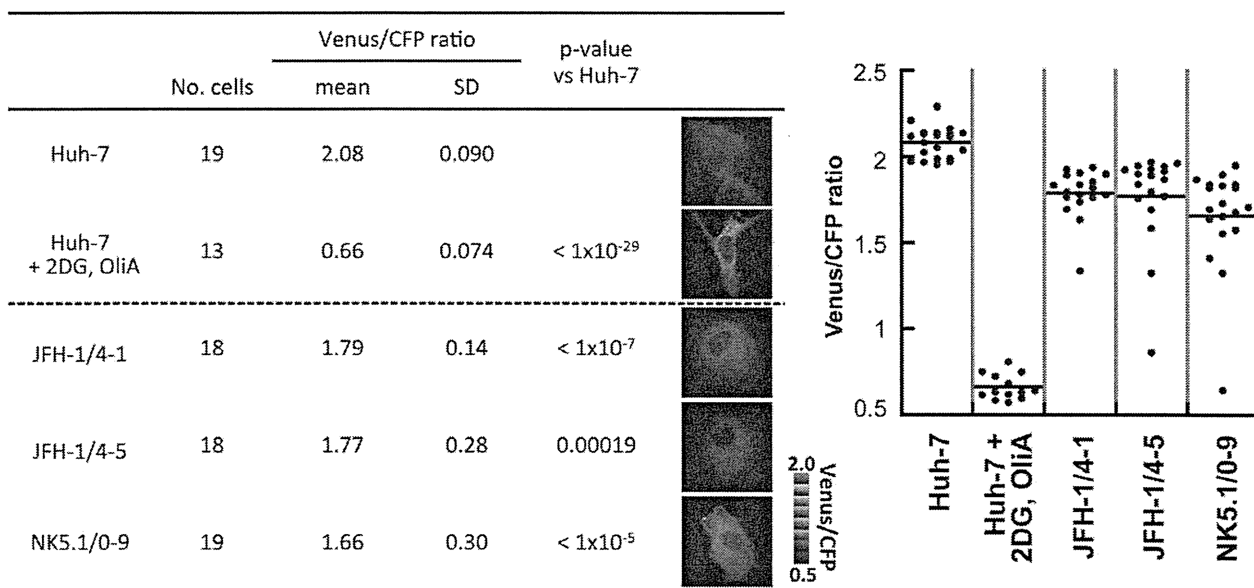

	No. cells	Venus/CFP ratio mean	Venus/CFP ratio SD	p-value vs Huh-7
Huh-7	19	2.08	0.090	
Huh-7 + 2DG, OliA	13	0.66	0.074	< 1x10^{-29}
JFH-1/4-1	18	1.79	0.14	< 1x10^{-7}
JFH-1/4-5	18	1.77	0.28	0.00019
NK5.1/0-9	19	1.66	0.30	< 1x10^{-5}

Figure 2. ATP fluctuations within the cytoplasm of HCV replicating cells analyzed using the original ATeam. Huh-7 cells carrying a HCV subgenomic replicon, JFH-1/4-1, JFH-1/4-5 (genotype 2a), and NK5.1/0-9 (genotype 1b) and parental Huh-7 cells were transfected with an ATP probe, AT1.03$^{\mathrm{YEMK}}$. Forty-eight hours after transfection, the Venus/CFP emission ratio in the cytoplasm of each cell was calculated from fluorescent images acquired with a confocal microscope FV1000 (Olympus). Huh-7 cells treated with 10 mM 2-DG and 10 µg/ml OliA for 20 min were used as a negative control. Data are presented as means and standard deviation values (SD) for each cell. Statistical differences among Huh-7 cells were evaluated using Student's *t*-test. Pseudocolored images of Venus channel/CFP channel ratios of representative cells and a pseudocolor scale are shown. In the graph on the right, each plot indicates the Venus/CFP ratio of each cell. The horizontal lines in the center represent the mean values for each group.
doi:10.1371/journal.ppat.1002561.g002

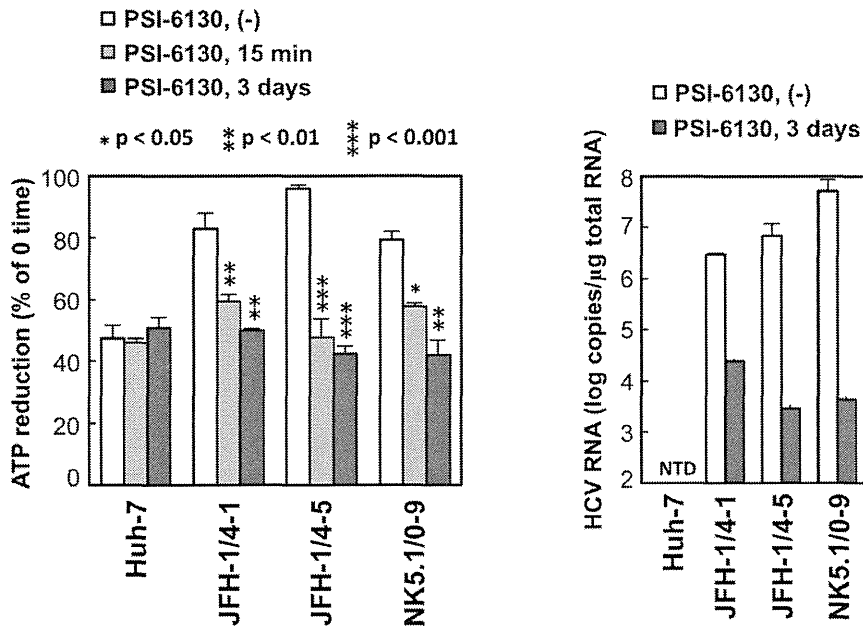

Figure 3. ATP consumption in cells replicating HCV RNA. (Left) The indicated cell lines were pretreated with 10 μM PSI-6130 for 3 days or were cultured in the absence of the drug, followed by trypsinization and permeabilization. ATP-containing reaction buffer plus 10 μM PSI-6130 was added to some of the non-pre-treated cells (PSI-6130, 15 min; light gray bars). ATP-containing PSI-6130-free reaction buffer was added to the rest of the non pre-treated cells (PSI-6130, (−); white bars) and to the pre-treated cells (PSI-6130, 3 days; dark gray bars). After 15 min incubation, ATP levels in cell lysates were measured using a luciferase-based assay. ATP reduction compared to ATP levels at the 0-time point was calculated. The mean values of three independent samples with SD are displayed. Statistical differences between cells treated with and without treatment with PSI-6130 were evaluated using Student's *t*-test. (Right) HCV RNA titers in cells corresponding to the left panel were determined using real-time quantitative RT-PCR. Data are presented as means and SD for three independent samples. NTD indicates not detected.
doi:10.1371/journal.ppat.1002561.g003

well as plasmids expressing NS5A-ATeam fusion proteins (NS5A-ATeam)(Figures 4A and 4C).

We first tested whether NS5A-ATeam fusion proteins can be used to monitor ATP levels over a range of concentrations in living cells. The Venus/CFP ratios in individual cells expressing NS5A fused either with AT1.03^{YEMK} ($Kd = 1.2$ mM at 37°C [2]) or with a relatively lower affinity version, AT1.03 ($Kd = 3.3$ mM at 37°C [2]) were measured. As shown in Figure 4B, differences in the Venus/CFP ratios of NS5A- AT1.03^{YEMK} and NS5A-AT1.03 were similar to those of AT1.03^{YEMK} and AT1.03, although average ratios were lower for NS5A- AT1.03^{YEMK} and NS5A-AT1.03 compared to AT1.03^{YEMK} and AT1.03. In the presence of 2DG and OliA, Venus/CFP ratios of NS5A-AT1.03^{YEMK} were markedly reduced to levels that were comparable to those of AT1.03^{RK}, an inactive mutant with R122K/R126K substitutions [2]. These results demonstrate that NS5A-ATeams can function as ATP indicators, although their dynamic ranges of Venus/CFP ratios are slightly smaller than those of the original, non-fused ATeams.

We next investigated whether the SGR-ATeam could initiate and sustain transient replication of HCV RNA in cells. A RNA polymerase I (Pol I)-derived plasmid, which carries SGR/luc-AT1.03 containing a luciferase reporter gene ([26]; Figure 4C), or its replication-defective mutant were transfected into Huh-7 cells and levels of viral replication were determined by measuring luciferase activity at various time intervals over a five day period (Figure 4D). Although replication of SGR/luc-AT1.03 was delayed compared with parental SGR/luc, the luciferase activity expressed from SGR/luc-AT1.03 rose to approximately a thousand-fold higher than that expressed from SGR/luc-GND-AT1.03 at five days post-transfection. It appears that SGR-AT1.03, which does not carry the luciferase gene, replicated more efficiently than SGR/luc-AT1.03, as determined by Western blotting of the HCV NS5B protein within cells four days post-transfection (Figure 4E). As indicated in Figure 4F, an abundant protein of the same size as that expected for the NS5A-ATeam fusion protein was observed in cells expressing either NS5A-AT1.03 or SGR-AT1.03, indicating that the NS5A-ATeam fusion protein is stable and is not cleaved during HCV replication. Thus, we concluded that the modified replicon constructs in which the ATeam is incorporated into the NS5A region are functional and remain capable of efficient transient replication of HCV RNA.

Visualization of ATP levels and distinctive features of ATP distribution in cells replicating ATeam-tagged SGR

This SGR-ATeam system that was established to analyze cellular ATP levels was used in living HCV RNA-replicating cells in which membrane-associated RCs are formed through the interaction of viral proteins, including NS5A, and cellular proteins. We compared the subcellular distribution of fluorescent signals expressed from NS5A-ATeams and SGR-ATeams using emission-scanning confocal fluorescence microscopy with a Zeiss META detector. NS5A-AT1.03 and NS5A-AT1.03^{YEMK} were diffusely distributed throughout the cytoplasm (Figure 5A; upper panels). Venus/CFP ratios of NS5A-ATeam constructs were almost constant throughout the cytoplasm (Figure 5A; lower). As expected, Venus/CFP ratios in cells expressing NS5A-AT1.03^{YEMK} were markedly higher than those of NS5A-AT1.03 (Figure 5A; lower). In contrast, cells replicating SGR-AT1.03 and SGR-AT1.03^{YEMK} showed foci of brightly fluorescent dot-like structures in the cytoplasm (Figure 5B; upper panels). Interestingly, some of these fluorescent foci had an apparently higher Venus/

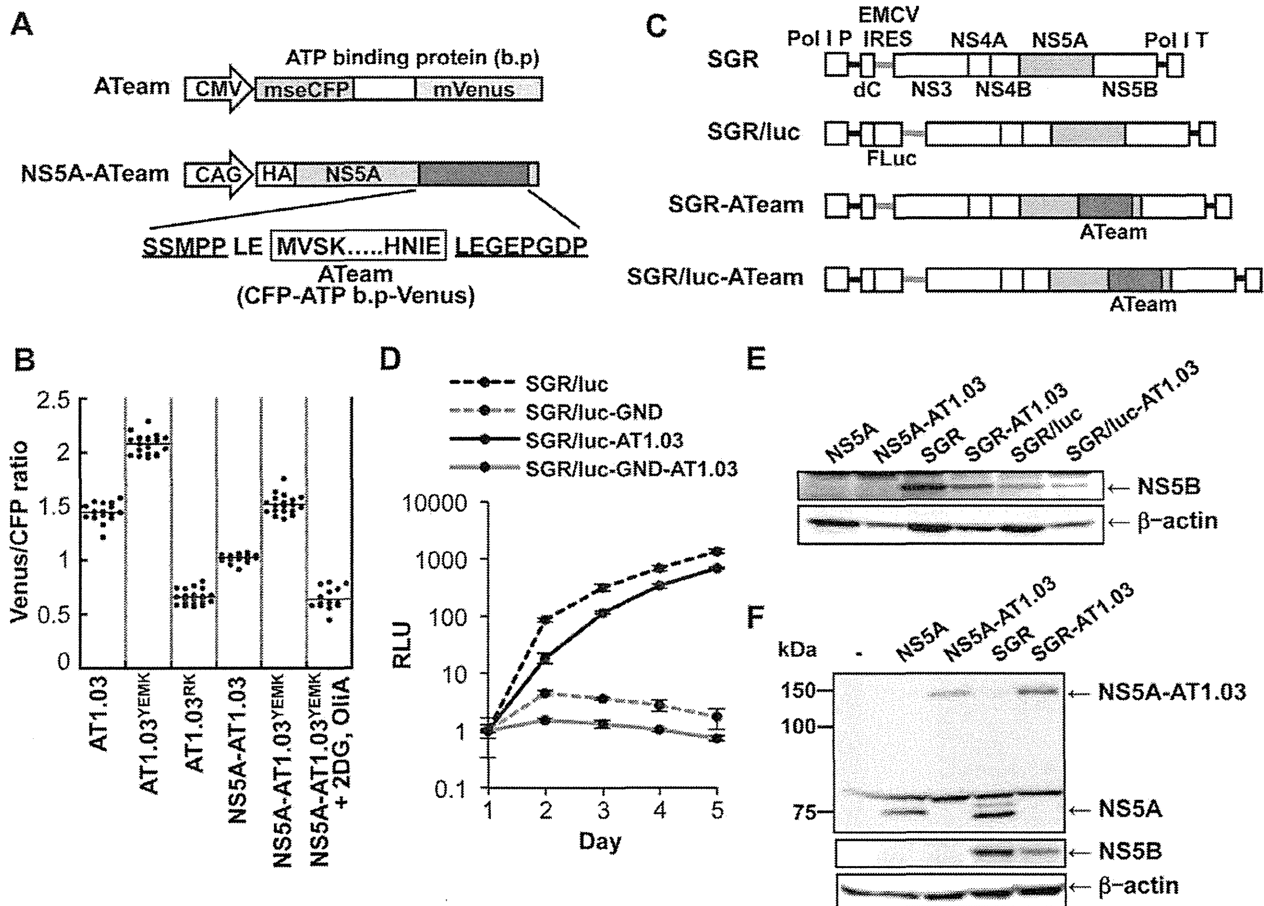

Figure 4. Development of NS5A-ATeam and SGR-ATeam to enable real-time monitoring of ATP. (A) Schematic representation of the ATeam and NS5A-ATeam used in this study. ATeam genes were inserted into the 3′ region of a HA-NS5A expression vector to generate NS5A-ATeam. The underlined sequences indicate NS5A residues. The insertion site was between residues 2394 and 2395, numbered according to the polyprotein of the HCV JFH-1 isolate. CMV, Cytomegalovirus promoter; CAG, CAG promoter; ATP b.p, ATP binding protein. HA, HA tag. (B) Huh-7 cells were transfected with ATeam and NS5A-ATeam constructs. Forty-eight hours post-transfection, the Venus/CFP ratios of each cell were calculated from fluorescent images acquired with a confocal microscope in the same way as described in the legends for Figure 2. Each plot shows the ratio of individual cells. Horizontal lines represent means. (C) Schematic representation of the SGR and SGR-ATeam plasmids used, with or without the firefly luciferase gene (Fluc). HCV polyproteins are indicated by the open boxes. ATeam genes were inserted into the same site in the NS5A C-terminal region. Bold lines indicate the HCV UTR. EMCV IRES is denoted by the gray bars. Pol I P, Pol I promotor; dC, 5′ region of Core gene; Pol I T, Pol I terminator. (D) Replication levels of SGR/luc-AT1.03 in transfected cells were determined by luciferase assay 1–5 days post-transfection. SGR/luc and SGR/luc-GND were used as positive and negative controls, respectively. Values given were normalized for transfection efficiency with luciferase activity determined 24 h post-transfection. All data are presented as means and SD for three independent samples. (E) Huh-7 cells were transfected with constructs encoding NS5A, NS5A-AT1.03, SGR, SGR-AT1.03, SGR/luc or SGR/luc-AT1.03, followed by immunoblotting with anti-NS5B or anti-beta-actin antibody. (F) Cells transfected with constructs encoding NS5A, NS5A-AT1.03, SGR or SGR-AT1.03 were analyzed by immunoblotting with anti-NS5A, anti-NS5B or anti-beta-actin antibodies.
doi:10.1371/journal.ppat.1002561.g004

CFP ratio than the surrounding cytoplasmic region (Figure 5B; middle and lower panels). Although the number of high Venus/CFP ratios was not consistent between the cells, this phenotype was observed in most of the cells that were replicating SGR-AT1.03 (Figure S3). Such high focal Venus/CFP ratios were not detected in cells replicating SGR-AT1.03^{RK} or in SGR-AT1.03^{YEMK} -replicating cells treated with 2DG and OliA. Thus, foci with a high Venus/CFP ratio apparently represent the presence of high ATP levels at distinct sites in cells replicating HCV RNA. In addition, when a replication-defective polyprotein that extended from NS3 through to the NS5B protein, including NS5A-AT1.03, was expressed, no high Venus/CFP ratio was seen in the cells in spite of the fact that NS5A-AT1.03 was detected in dot-like structures throughout the cytoplasm (Figure S4). These results strongly suggest that the high Venus/CFP ratios observed using the SGR-ATeam system are associated with the replication of HCV RNA.

To investigate whether the high Venus/CFP ratios of the dot-like structures detected in cells replicating SGR-ATeam are located at the HCV RC, FRET images of SGR-AT1.03-replicating cells were analyzed, followed immunofluorescence analysis of cells fixed and stained with either anti-NS5A or anti-NS3 antibodies (Figure 5C). Confocal fluorescence microscopy at high magnification demonstrated that the high Venus/CFP ratios that were identified in foci of various sizes were co-localized with NS5A and NS3 that were possibly membrane-bound within the cytoplasm of the viral replicating cells. Some of the NS3- or NS5A-labeled proteins that were identified by immunofluorescence were not associated with high Venus/CFP ratios. These results are consistent with previous reports, which demonstrated that only

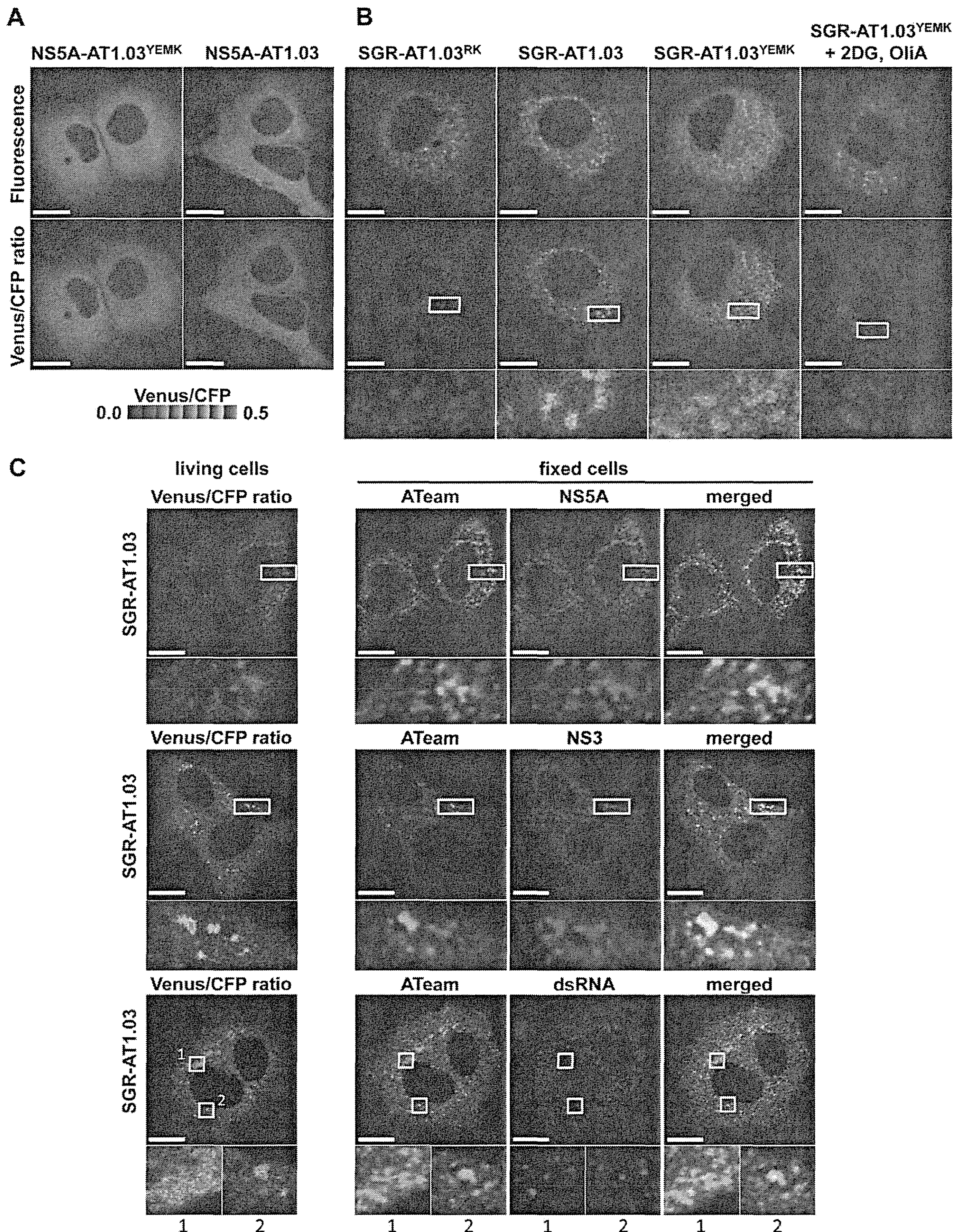

Figure 5. Visualization of sites of focal accumulation of ATP in cells expressing NS5A-ATeam or SGR-ATeam. (A) Huh-7 cells were transfected with NS5A-AT1.03 or NS5A-AT1.03^{YEMK}. Four days after transfection, the cells were analyzed using spectral imaging (405-nm excitation) of LSM510-META (Carl Zeiss). Images were processed to the CFP channel (F_{CFP}) and the Venus channel (F_{Venus}) using a linear unmixing algorithm using a reference for each spectrum. The upper panels demonstrate the signal intensity from a spectral channel with maximum intensity and represent the expression pattern of NS5A-ATeam. The lower panels are constructed from FRET ratio images (F_{CFP}/F_{Venus}) with pseudocolors. The pseudocolor scale is shown below. Scale bars, 20 μm. (B) Huh-7 cells were transfected with SGR-AT1.03^{RK}, SGR-AT1.03 or SGR-AT1.03^{YEMK}, and were analyzed in the same

way as described in (A). SGR-AT1.03^{YEMK} -transfected cells were treated with 10 mM 2DG and 10 μg/ml OliA just before imaging and were used as a negative control. The upper panels demonstrate the intensity from a spectral channel with maximum intensity and represent the expression pattern of NS5A-ATeam processed from SGR-ATeam. The lower panels indicate square areas within FRET ratio panels magnified five-fold. Scale bars, 20 μm. (C) Cells were fixed after live-cell FRET imaging, and the same cell was analyzed by indirect immunofluorescence staining. Viral proteins were labeled with antibodies against NS5A (upper panels), NS3 (middle panels) and dsRNA (lower panels), which were detected with an Alexa Fluor 555-labeled anti-rabbit or anti-mouse antibody. ATeam panels (green) represent the expression of NS5A-ATeam processed from SGR-ATeam, and NS5A, NS3 or dsRNA panels (red) represent the immunostained signals. Enlarged views of the areas outlined by squares at a five-fold magnification are also shown. Scale bars, 20 μm.
doi:10.1371/journal.ppat.1002561.g005

some of the expressed HCV NS proteins contribute to viral RNA synthesis [27]. To further investigate the relationship between the cellular sites at which there was a high Venus/CFP ratio and HCV RNA replication, double-stranded RNA (dsRNA) was visualized by staining with a specific anti-dsRNA antibody after FRET imaging (Figure 5C). This staining indicated that dsRNA-containing dot-like structures co-localized with structures that displayed high Venus/CFP ratios. Therefore, it is most likely that the dot-like structures with high Venus/CFP ratios that were detected using the SGR-ATeam system reflect the sites of HCV RNA replication or HCV RCs.

Several studies have shown that mitochondria, which play a central role in ATP metabolism, localize to areas near the membranous web, the likely site of HCV RNA replication [28]. We thus compared the subcellular localization of the fluorescence signals detected in cells expressing SGR-ATeam with that of mitochondria that were visualized by staining with Mitotracker. Foci with high Venus/CFP ratios did not colocalize with, but were localized adjacent to mitochondria in cells that were replicating SGR-AT1.03 (Figure S5). This finding might reflect the fact that ATP can be directly supplied from mitochondria to the sites of viral RNA replication in cells.

Quantification of ATP at putative cytoplasmic sites of HCV RNA replication within cells

Based on the above observations, FRET signals detected within cells expressing SGR-ATeam or NS5A-ATeam can be classified as either signals from distinct dot-like structures, which represent putative subcellular sites of HCV RNA replication, or as signals that are diffuse throughout the cytoplasm. The Venus/CFP emission ratio in individual cells into which NS5A-AT1.03, NS5A-AT1.03^{YEMK}, SGR-AT1.03, SGR-AT1.03^{YEMK} or SGR-AT1.03^{RK} was introduced was determined (Figure 6A). Fluorescent signals corresponding to cytoplasmic ATP were identified by subtracting signals at putative sites of viral RNA replication from signals from the cytoplasmic area as a whole. Cytoplasmic Venus/CFP ratios within cells replicating SGR-AT1.03 and SGR-AT1.03^{YEMK} were lower than those in cells expressing NS5A-AT1.03 and NS5A-AT1.03^{YEMK}, respectively. Therefore, cytoplasmic ATP levels within HCV RNA-replicating cells were lower than in non-replicating cells. This result is consistent with the findings shown in Figure 1A. The average Venus/CFP ratios at potential sites of viral RNA replication were greater than the corresponding cytoplasmic levels in cells replicating SGR-AT1.03 or SGR-AT1.03^{YEMK}. As expected, a significant decrease in Venus/CFP ratios was observed in cells treated with 2DG and OliA.

We next quantified ATP levels within individual cells replicating HCV RNA based on the Venus/CFP ratios obtained. To generate standard curves for this calculation, permeabilized cells expressing NS5A-AT1.03 or NS5A-AT1.03^{YEMK} were prepared by digitonin treatment, followed by the addition of defined concentrations of ATP and subsequent FRET analysis [29,30]. As shown in Figure 6B, under these experimental conditions, baseline Venus/CFP ratios of approximately 0.1 were detected in the absence of exogenous ATP, and Venus/CFP ratios were observed to increase linearly with increasing ATP concentration. The standard curves thus obtained can be used to estimate the ATP concentrations of unknown samples in which a particular ATeam containing an ATP probe at the C terminus of HCV NS5A, such as NS5A-ATeam or SGR-ATeam, have been introduced. Based on the fluorescent signal obtained in cells replicating SGR-ATeam, as well as in cells expressing NS5A-ATeam, the ATP concentration at putative sites of HCV RNA replication was estimated to be ~5 mM in the experiments shown in Figures 5A and 5B (average value of putative replication sites; 4.8 mM). After subtraction of the ATP that was localized at the HCV replication sites, the ATP concentration of HCV-replicating SGR cells (~1 mM) was found to be approximately half that observed in parental non-replicating cells (~2 mM)(average values in SGR and parental cells; 0.8 mM and 2.2 mM, respectively). To our knowledge, this is the first experiment in which ATP levels were estimated inside living cells during viral genome replication.

Figures 5 and 6A demonstrate changes in ATP concentrations at distinct sites in cells undergoing HCV RNA replication. Finally, we determined the effect of the PSI-6130 inhibitor of HCV replication on the change in subcellular ATP concentration in cells following introduction of SGR-AT1.03, SGR-AT1.03^{RK} or NS5A-AT1.03 (Figure 6C). In general, nucleoside analogue inhibitors of viral replication prevent RNA/DNA synthesis by chain termination immediately after addition to infected cells [23]. Indeed, as shown in Figure 3, a decrease in ATP consumption was detected even following a PSI-6130 treatment period as short as 15 min of permeabilized HCV replicon cells. We therefore analyzed and estimated ATP levels in cells in the presence of PSI-6130 for 10 min and 2 h. ATP concentrations at putative sites of viral RNA replication, as well as cytoplasmic ATP levels, were higher in SGR-AT1.03-replicating cells in the presence of 0.1–5 μM PSI-6130 for 10 min compared to the same cells without inhibitor treatment or to NS5A-AT1.03-expressing cells. A dose-dependent PSI-6130-induced increase in ATP levels at the putative replication sites was observed under the condition used. By treatment with PSI-6130 for 2 h, the ATP levels at putative replication sites were significantly lower than those without inhibitor treatment in SGR-AT1.03-replicating cells. The cytoplasmic ATP levels were similar with or without 2-h treatment (Figure 6C). In HCV SGR-ATeam cells treated with PSI-6130 for 3 days, HCV RNA replication was dramatically inhibited by greater than 90% with no observed cytotoxicity (Figure S6) and, as expected, little or no high Venus/CFP signal was detected anywhere in the cells (data not shown). We adapted the ATeam system to monitor ATP in HCV RNA replicating cells and found increased ATP levels at the putative subcellular sites of the viral replication. Findings obtained from experiments using the viral polymerase inhibitor strongly suggest that changes in ATP concentrations at the distinct sites observed depend on the viral RNA replication.

Discussion

This paper is the first to demonstrate changes in ATP within cells during viral genome replication. ATP requirements during

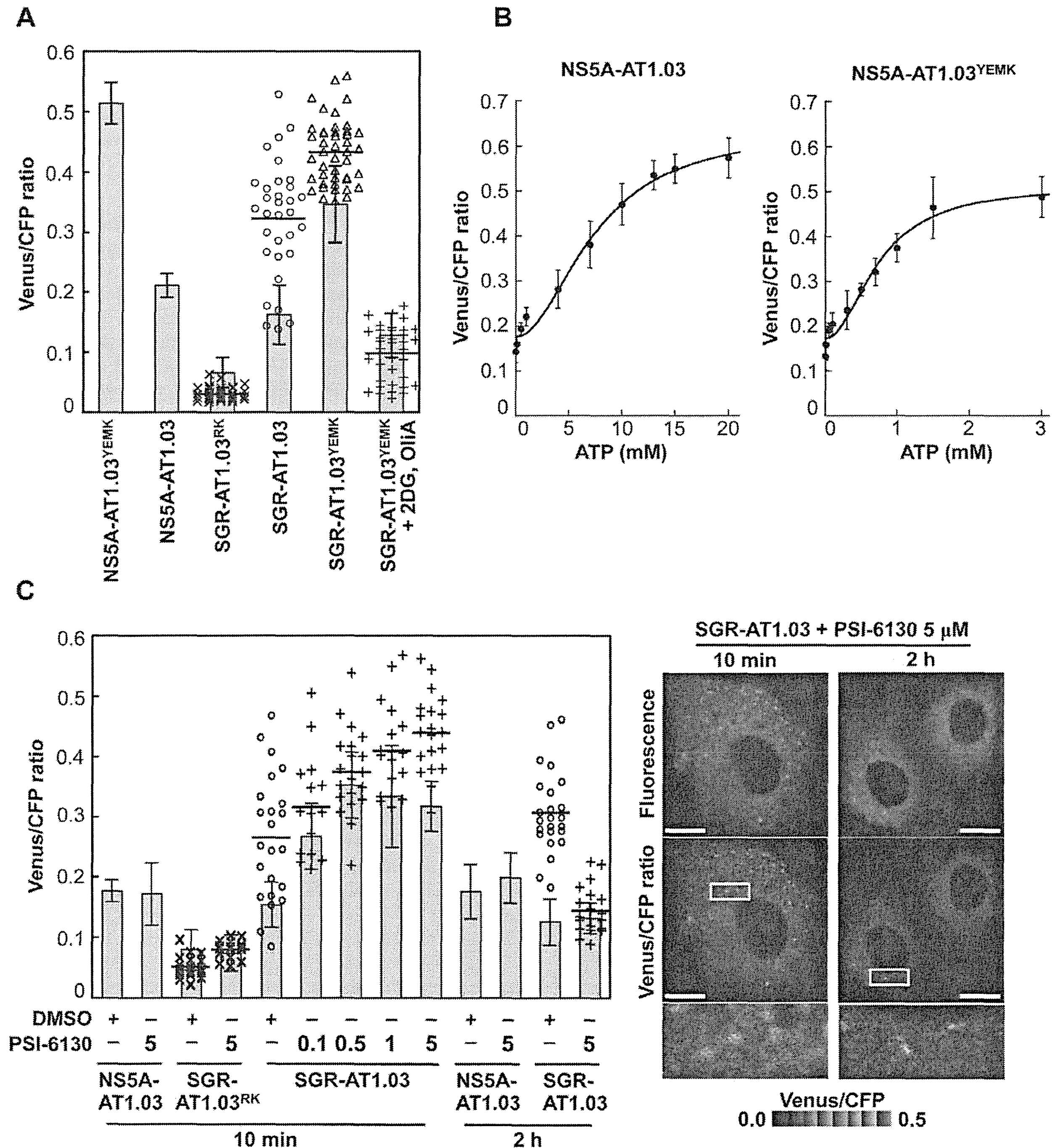

Figure 6. Estimation of ATP levels at possible sites of HCV RNA replication in living cells. (A) Venus/CFP emission ratios were calculated from images of CFP and Venus channels in individual cells for each group. Bar- and dotted graphs indicate ratios within the cytoplasm and ratios for dot-like structures, respectively, in the same cells, as shown in Figures 5A and 5B. Data in bar graphs are indicated as means and SD. Horizontal lines in the dot graphs denote means from at least three independent cells. Values in the cytoplasm of cells transfected with NS5A-AT1.03^{YEMK} and SGR-AT1.03^{YEMK} were statistically significant ($p<0.05$) as evaluated using the Student's *t*-test. (B) Calibration of NS5A-ATeam in cells under semi-intact conditions. Cells were transfected with NS5A-AT1.03 and NS5A-AT1.03^{YEMK}, respectively. Forty-eight hours later, the cells were permeabilized, followed by addition of known concentrations of ATP. FRET analyses were performed as described in Figure 5A. Each trace represents mean with SD of at least six independent cells. Plots were fitted with Hill equations with a fixed Hill coefficient of 2; $R=(R_{max}-R_{min})\times[ATP]^2/([ATP]^2+Kd^2)+R_{min}$, where R_{max} and R_{min} are the maximum and minimum fluorescence ratios, respectively. *Kd* is the apparent dissociation constant. R values were 0.994 and 0.986 for NS5A-AT1.03 and NS5A-AT1.03^{YEMK}, respectively. (C) Cells were transfected with NS5A-AT1.03, SGR-AT1.03^{RK} or SGR-AT1.03. The cells were then treated with PSI-6130 at indicated concentrations (μM) for 10 min or 2 h, and were analyzed as described in (A). Values in the cytoplasm of cells transfected with SGR-AT1.03 with and without PSI-6130 treatment were statistically significant ($p<0.05$ for control versus 0.1 or 1 μM PSI-6130, $p<0.01$ for control versus 0.5 or 5 μM PSI-6130) as evaluated using the Student's *t*-test. Representative cells treated with 5 μM PSI-6130 are shown in the right panel. The lower panel is a five-fold magnification of the boxed area. Scale bars, 20 μm.
doi:10.1371/journal.ppat.1002561.g006

the virus lifecycle have been studied for years. Several key steps during the viral life cycle, such as genome synthesis, require high-energy phosphoryl groups. For instance, it has been shown that ATP is required for the formation of a preinitiation complex for de novo RNA synthesis by RdRp of flaviviruses [31]. Transcriptional initiation and RNA replication by influenza virus RdRp are functional in an ATP-dependent fashion [32,33]. An ATP requirement of viral helicase activities has also been reported [34]. Furthermore, it has been demonstrated that ATP is involved in the assembly and/or release of viral structural proteins possibly via interaction with ATP-dependent chaperones [35,36]. However, it has been controversial as to whether ATP can be concentrated in particular subcellular compartment(s) in infected cells during viral replication. One of the underlying reasons for this controversy may be that a method by which cellular ATP levels can be determined, apart from examination of ATP levels in cellular extracts in the steady-state, has been lacking [37]. Recently Imamura et al. established FRET-based indicators, known as ATeams, for ATP quantification, and have shown that the use of ATeams enables the monitoring of ATP levels in real-time in different cellular compartments within individual cells [2].

In this study, in order to visualize and monitor ATP levels in living cells during replication of the viral genome, we first introduced the original ATeam-expressing plasmids into cells and found that cytoplasmic ATP levels in cells undergoing HCV genotype 1b and 2a RNA replication were lower than those in cured or parental cell lines (Figures 2 and S2). These results agree with the results of CE-TOF MS analysis (Figure 1) and the ATP consumption assay (Figure 3). It is therefore likely that ATP is actively consumed in cells during viral RNA replication, resulting in reduced levels of ATP in the cytoplasm. Furthermore, NS5A-ATeam fusion constructs, in which the ATeam gene was introduced into the C-terminal end of the NS5A coding region, and SGR-ATeam constructs containing a HCV JFH-1-derived subgenomic replicon within the NS5A-ATeam fused sequence as described above, were engineered (Figure 4). The results obtained using several ATeam fusion constructs with different affinities for ATP indicated that NS5A-ATeam fusion constructs can be used as FRET-based ATP indicators, and that the ATeam-tagged HCV replicons are capable of transient replication of viral RNA (Figure 4). It is interesting that our experiment using a SGR-ATeam construct provides evidence for the formation of ATP-enriched foci within cells that support HCV RNA replication (Figures 5 and 6). FRET-signal detection followed by indirect immunofluorescence allowed us to visualize co-localization of viral proteins as well as dsRNA at sites of ATP accumulation in cells (Figure 5), suggesting that these membrane-associated ATP-enriched foci likely represent sites of HCV RNA replication in transient replication assays.

Attempting to precisely quantify ATP within individual cells or particular intracellular compartments is a very challenging process. The luciferin-luciferase reaction has been utilized to monitor cellular ATP levels by measuring the released photon count during catalysis of bioluminescent oxidation by firefly luciferase. A previous study based on the luciferin-luciferase assay estimated basal cytoplasmic ATP levels at ~1.3 mM, which increased to ~5 mM during apoptotic cell death [38]. However, the results obtained were likely influenced by cellular levels of luciferase and other assay components, as well as by the pH of the cells. In this study, we describe quantification of ATP in human hepatoma Huh-7 cells undergoing HCV RNA replication using SGR-ATeam technology. Although ATP requirements during the lifecycles of various viruses have been studied for years, the use of ATeam technology enabled us, for the first time, to evaluate ATP concentrations at sites of viral replication within living cells. We here demonstrate that ATP concentrations at these putative subcellular sites of HCV RNA replication approach ~5 mM (Figure 6). This ATP level is as high as that observed during apoptotic processes such as caspase activation and DNA fragmentation, even though the latter ATP level was determined using a different assay system [38]. Considering that these apoptotic events were not observed at basal ATP levels [38], replication of the viral genome likely also requires high concentrations of cellular ATP. It should be noted that, in contrast to the fluorescent reporter system traditionally used to calculate the ATP/ADP ratio [39], the bacterial epsilon subunit used in ATeam is highly specific for ATP, but not for other nucleotides such as ADP, CTP, GTP or UTP [2,3]. In evaluating the effect of the HCV polymerase inhibitor on changes in the subcellular ATP concentration in cells replicating SGR-ATeam, an increase in ATP concentration was observed both at putative replication sites and in the cytoplasm of SGR-AT1.03-replicating cells in the presence of PSI-6130 for 10 min (Figure 6C). By contrast, 2-h treatment with the inhibitor resulted in reduction of ATP levels at putative replication sites in the replicon cells. Although the result of the experiment with 10-min treatment may be somewhat unexpected, it might possibly be explained by the following hypothesis. PSI-6130 began to inhibit viral RNA synthesis, leading to a decrease in ATP consumption. Since a mechanism for ATP transport mediated by host cell and/or viral factor(s) is still active during this time period, the ATP level at the replication sites should be increased compared to that during active replication. Higher levels of metabolic intermediates for glyconeogenesis as well as for glycolysis in HCV-infected cells compared to non-infected cells as determined via metabolome analysis (data not shown) may also be implicated in the increased ATP levels at the initial stage of inhibition of HCV replication. It is likely that active consumption of ATP caused by HCV replication and ATP transportation into the replication sites would lead to reduction of cytoplasmic ATP level. Such a change in ATP balance may result in induction of ATP generation and increase in certain metabolic intermediates related to glucose metabolism. These metabolome responses are supposed to maintain in short-term (10 min) treatment with PSI-6130. Thus, inhibition of HCV RNA replication by PSI-6130 under the conditions used may lead to increase in the cytoplasmic ATP level. It is likely that these metabolome responses were not observed after the longer-term (2 h) treatment presumably because the viral replication was inhibited by the inhibitor for a sufficient period of time. Further study is required to address the molecular mechanism underlying change in ATP balance caused by HCV replication and the viral inhibitors.

The mechanism by which ATP accumulates at potential sites of HCV RNA replication remains unclear. We have previously demonstrated that creatine kinase B (CKB), which is an ATP-generating enzyme and maintains cellular energy stores, accumulates in the HCV RC-rich fraction of viral replicating cells [22]. Our earlier results suggest that CKB can be directed to the HCV RC via its interaction with the HCV NS4A protein and thereby functions as a positive regulator for the viral replicase by providing ATP [22]. One may hypothesize that recruitment of the ATP generating machinery into the membrane-associated site, through its interaction with viral proteins comprising the RC, is at least in part linked with elevated concentrations of ATP at a particular site. Through our preliminary study, however, subcellular ATP distribution was not changed significantly in replicon cells where HCV RNA replication was reduced ~50% by siRNA-mediated knockdown of the CKB gene (data not shown). Another possibility